

FAST REACTOR KINETICS - THE QXI CODE

by

D.A. Meneley, K.O. Ott,  
and E.S. Wiener

March 1971

## TABLE of CONTENTS

ABSTRACT .....	6
I. INTRODUCTION .....	6
II. CAPABILITIES AND LIMITATIONS .....	8
III. EQUATION SET .....	11
A. Problem-setup Module .....	11
1. Cross Sections.....	11
2. Group Collapsing .....	14
3. Transverse Bucklings .....	15
B. Steady-state Module .....	15
1. Steady-state Equations.....	16
2. Criticality Search.....	18
3. Adjoint Solution.....	19
4. Normalization.....	19
C. Dynamic Module .....	20
1. Time-dependent Equations.....	21
2. Initial Conditions .....	23
3. Sequence of Solution.....	24
4. Numerical Approximations.....	28
5. External Sources; First-collision Distributions .....	30
IV. TIME-STEP SELECTOR .....	32
A. Reactivity Recalculation Steps.....	32
B. Shape-function Recalculation Steps .....	33
1. Inverse-period Test.....	34
2. Preset Time Steps .....	34
3. Shape-function Change Test .....	34
4. Delayed-neutron Source Test.....	35
5. Coolant-velocity Test .....	35
6. Regionwise-reactivity Test.....	35
7. Amplitude-function Test.....	35
8. Tightening Convergence near Prompt Critical .....	36

V. DRIVING FUNCTIONS.....	37
A. Triggering.....	37
B. Mixture Modifiers.....	38
C. Shape-function Step Controller .....	38
D. Source Modifiers .....	38
E. Modifier Data.....	39
F. Time Look-ahead .....	39
VI. INPUT PREPARATION.....	40
A. Input-card Formats and Data Descriptions.....	40
1. Title Card.....	40
2. Parameter and Control Card.....	40
3. Delayed-neutron Precursor Data .....	41
4. Isotope-to-Mixture Specifications.....	42
5. Cross-section File Preparation Cards .....	43
6. Mixture-to-Composition Specification .....	43
7. Fixed-point Relative-addressed Data.....	44
8. Floating-point Relative-addressed Data.....	47
9. Driving-function Specifications.....	51
10. Feedback Data .....	53
11. Problem End Card .....	54
B. Sample Problems.....	54
1. Test Problem 1 .....	54
2. Test Problem 2 .....	57
VII. OUTPUT .....	61
A. Printed Output.....	61
B. Permanent Files .....	62
1. Amplitude Data .....	62
2. Shape-function Data .....	62
VIII. FUEL-TEMPERATURE CALCULATION .....	63

IX. QX1 CROSS-SECTION FILE.....	64
A. Card Input .....	64
B. Structure and Content of Cross-section File .....	66
C. Limitations on Cross-section File .....	68
X. SCRATCH FILES .....	70
A. Logical Unit 03 .....	70
B. Logical Unit 04 .....	73
C. Logical Unit 08 .....	74
D. Logical Unit 09 .....	74
E. Logical Unit 10 .....	74
F. Logical Unit 50 .....	74
XI. SUBROUTINE DESCRIPTIONS .....	77
XII. PROGRAM STRUCTURE.....	81
XIII. COMMON BLOCK DICTIONARY.....	87
ACKNOWLEDGEMENTS.....	102
REFERENCES .....	103

## LIST OF FIGURES

<u>No.</u>	<u>Title</u>	<u>Page</u>
1.	Time-step Sequence .....	25
2.	DRIVER Calling Sequence.....	83
3.	SETUP Calling Sequence .....	84
4.	STATIC Calling Sequence .....	85
5.	DYNAM Calling Sequence .....	86

## LIST OF TABLES

<u>No.</u>	<u>Title</u>	<u>Page</u>
I.	Physical-model Assumptions .....	8
II.	Maximum Dimensions .....	9
III.	Sequence of Steps during Setup and Steady-state Calculations .....	16
IV.	Sequence of Steps during Dynamic Calculation .....	20
V.	Time-step Convergence Criteria .....	49
VI.	Test Problem 1 .....	55
VII	Test Problem 2 .....	57
VIII	QX1 Subroutine .....	77
IX.	Major Program Control Flags .....	81

# FAST-REACTOR KINETICS—THE QX1 CODE

By

D.A. Meneley, K.O. Ott,\*  
And E.S. Wiener

## ABSTRACT

This report describes the QX1 code (Quasistatic Excursion Code, 1-dimensional). The code solves the transient, one-dimensional, multigroup diffusion equations by factorizing the total flux into a time-dependent amplitude function and a space-energy-time-dependent shape function. The capability of modifying resonance cross sections as a function of fuel temperature to account for Doppler feedback has been included. The model was specifically designed for extension to two space dimensions and for inclusion of further feedback algorithms to describe thermal-hydraulic and other effects, though these models were not included as part of this development.

## I. INTRODUCTION

This report is primarily a computer-code description and therefore does not present the QX1 factorization method as a complete picture. The basic idea appears in Ref. 1; it drew on material developed in Ref. 2. Various features and performance descriptions can be found in annual reports of the ANL Reactor Physics Division<sup>3-6</sup> and ANS Transactions<sup>7,8</sup>. The primary reference is the Nuclear Science and Engineering paper.<sup>9</sup>

The code was developed on the CDC-3600 machine. It has been converted to the IBM 360/75 for incorporation into the ARC system.<sup>10</sup> Copies of both versions are available in the Argonne Code Center. Specifically, this report describes the code identified as "Edition 5, dated December 1, 1970."<sup>11</sup>

The limitations of one-dimensional methods for application to fast-reactor safety analysis are well known. These limitations have led to the conclusion that QX1 should not be developed into a full safety package. Instead, the code represents a completed methods-development activity whose product is ready for application to two- and three-dimensional safety-analysis systems. The two-dimensional development is discussed in Ref. 11.

In its present form, the code is useful for developing the necessary understanding of spatial kinetics phenomena in LMFBR's. Applications in this context are given in Refs. 12-20.

## II. CAPABILITIES AND LIMITATIONS

The neutron behaviour is approximated in the standard multigroup diffusion-theory model. Finite-differencing is identical to that of Ref. 21. One space dimension (slab, cylinder, sphere) may be treated. The assumptions made in the physical model are given in Table I; important dimension limits are listed in Table II.

TABLE I. Physical-model Assumptions

1. Multigroup diffusion theory can describe neutron balance.
  2. Prompt- and delayed-neutron emission spectra are independent of fissioning isotope and incident energy.
  3. Delayed-neutron yield per fission is independent of incident energy
  4. Neutron energy can only be decreased in scattering reactions.
  5. Group cross sections are independent of changes in density, spectrum, or temperature, with the exception of resonance capture and fission.
  6. Group cross sections for resonance capture and fission can be represented as functions of temperature, independent of changes in potential-scattering competition.
  7. The group macroscopic transport cross section can be represented as a linear combination of group microscopic transport cross sections. Temperature corrections to the microscopic cross sections are given by the sum of the changes in capture and fission cross sections relative to the reference temperature.
-

TABLE II Maximum Dimensions

Energy groups	30	Total mixtures in problem	
Scattering band (downscatter only)	15	Temperature-dependent	8
		Temperature-independent	8
Mesh intervals	149	Isotopes per mixture	20
Regions of different composition	20	Delayed-neutron precursor families	6
Mixtures per composition			
Temperature-dependent	8		
Temperature-independent	8		

The code reads cross sections from the XLIBIT<sup>22</sup> library file (CDC-3600 version only) or from the QX1 file. Up to eight mixtures may be formed with temperature-dependent capture, fission, and transport cross sections, using the method described in Ref. 3. The delayed-neutron data are read from cards. The model used is the incident-energy-independent yield formulation of Ref. 23. Details of the problem-setup module of the code are given in Section III.A.

Initial conditions are established either by one of several criticality searches or by a static external-source solution. The QX1 formulation requires the initial steady-state adjoint flux; this is found either for the critical condition resulting from the search or as the  $\lambda$ -mode solution in the system without external sources. The formulation for initially subcritical systems was developed in Ref. 4. Details of the steady-state module of the code are given in Section III.B.

The dynamic-solution module consists mainly of a time-step controller, a point-kinetics algorithm, a shape-function routine, a space-energy integration routine, an excursion-initiation system, and feedback routines. (The latter are somewhat skeletal.) Several iterative sequences are required in the three nested levels of time steps.

The method is amenable to inclusion of a variety of feedback models. One serious limitation is the fact that the mesh points are fixed in position. Thermal expansion, therefore, is difficult to simulate accurately. The second basic limitation is due to the single space dimension, in which it is quite difficult to

treat changes in the transverse direction. The QX1 code does not treat this problem. Details of the dynamic solution module are given in Section III.C.

Problem results at selected time points may be saved in a dump file for plotting and other manipulations. Various other minor options are described in the following sections.

### III. EQUATION SET

#### A. Problem-setup Module

##### 1. Cross Sections

Isotropic cross sections are provided from a library file. These are combined with specified atom densities to produce mixtures for a given problem. A mixture containing one or more fissionable isotopes may have temperature-dependent capture, fission, and transport cross sections (see details below). These mixtures are combined with specified volume fractions and temperatures to produce macroscopic cross sections for reactor regions, identified as compositions. The temperature and/or volume fraction of a given mixture in a region may be varied during the problem.

The temperature dependence is specified at the isotope level in the following manner. Four separate cross-section decks with the same five-character isotope label are input in the library-preparation routines. These four decks must be ordered by increasing temperature. The cross sections of the lowest-temperature isotope (the first of the four) are taken as the reference values. The reference temperature must be the same for all isotopes in the file. Capture and fission cross sections only are read from each of the other three decks; these are stored on the QX1 library file.

The first step of cross-section preparation is calculation of the mixture cross sections. These are obtained by reading the Mixture Data (see Section VI.A.4) and accumulating the product of the atom density of each isotope in each mixture with the isotope cross sections. For any temperature-independent mixture, the macroscopic cross sections of mixture  $m$  are given by:

$$\sigma_m^x = \sum_{i \in m} n_{i,m} \sigma_i^x, \quad (1)$$

where  $x$  represents any cross section of isotope  $i$ . For a mixture containing fissionable isotopes, capture and fission cross sections for each energy group are generated at each of four temperatures  $T_1, T_2, T_3$  and  $T_4$ :

$$\sigma_m^x(T_k) = \sum_{i \in m} n_{i,m} \sigma_i^x(T_k). \quad (2)$$

The sum extends over all isotopes in the mixture; the single cross sections given for non fissionable isotopes are used at all four temperatures.

The mixture cross-section interpolation coefficients  $a_m^{x,\ell}$  are then calculated for capture and fission cross sections in each group for each temperature-dependent mixture:

$$\sigma_m^x(T_k) = \sigma_m^x(T_1) + \int_{T_1}^{T_k} \left( \frac{a_{m,1}^x}{\sqrt{T}} + \frac{a_{m,2}^x}{T} + \frac{a_{m,3}^x}{T^2} \right) dT \quad (3)$$

The second term in the integrand represents the major  $1/T$  dependence; the first term gives  $1/T^{1/2}$  dependence at low energies, and the last term accounts for high-energy dependence with resonance overlap.

The  $a_m^{x,\ell}$  coefficients are saved for later calculation of mixture cross sections at intermediate temperatures by substitution in Eq. 3. The mixture transport cross section at temperature  $T$  is given by

$$\sigma_m^{tr}(T) = \sigma_m^{tr}(T_1) + [\sigma_m^c(T) - \sigma_m^c(T_1)] + [\sigma_m^f(T) - \sigma_m^f(T_1)]. \quad (4)$$

The temperature dependence of the prompt and delayed fission yields have been approximated to reduce storage requirements. For a given mixture in a given energy group, the prompt-neutron yield  $\nu_m^p$  and delayed-neutron precursor yield for family  $s, \nu_{m,s}^d$ , per fission are given by

$$\nu_m^p = \frac{\sum_{i \in m} n_{i,m} \nu_i^p \sigma_i^f(T_1)}{\sum_{i \in m} n_{i,m} \sigma_i^f(T_1)}$$

and

$$\nu_{m,s}^d = \frac{\sum_{i \in m} n_{i,m} \nu_{s,i}^d \sigma_i^f(T_1)}{\sum_{i \in m} n_{i,m} \sigma_i^f(T_1)}. \quad (5)$$

These values are then assumed to be temperature-independent for the remainder of the problem. This introduces an error because of the real variation of  $\nu_m^p$  and  $\nu_{m,s}^d$  with temperature which is a result of the averaging procedure. The error should be unimportant, because the temperature dependence of the fission cross section is confined to the energy range below about 25keV, where the contribution to the fission source is a small fraction of the total.

To reduce storage requirements, the  $(n,p), (n,\alpha),$  and  $(n,2n)$  cross sections are combined with capture and scattering during microscopic data processing. The “capture” cross section in each group is given by

$$\sigma_i^c = \sigma_i^{(n,\gamma)} + \sigma_i^{(n,p)} + \sigma_i^{(n,\alpha)} - \sigma_i^{(n,2n)} \quad (6)$$

The scattering matrix  $\sigma_{i,g'g}$  is given by

$$\sigma_{i,g'g} = \sigma_{i,g'g}^{(elastic)} + \sigma_{i,g'g}^{(inelastic)} + 2\sigma_{i,g'g}^{(n,2n)} \quad (7)$$

The subtraction of the  $(n, 2n)$  cross section in Eq. 6 is necessary because the code later calculates the macroscopic total group removal cross section from

$$\sigma^r = \sigma^c + \sigma^f + \sum_{g' > g} \sigma_{g'g} + \frac{1}{3\sigma^{tr}} B^2 \quad (8)$$

Composition specifications (see Section VI.A.6) are given for each different set of mixture volume fractions and temperatures. These specifications are taken as initial values and are duplicated in each region in which they are to appear. (See variable MIR(l) in Section VI.A.7.) Subsequent to problem setup, these duplicated compositions are considered to be independent, so that “composition” is 1:1 with “region”. The composition specification includes the initial temperature of each mixture. The initial mixture cross sections are interpolated to this temperature by means of Eqs. 3 and 4.

Composition cross sections at any time are computed by

$$\sigma_c^x(T, t) = \sum_{m \in c} F_{m,c}(t) \sigma_m^x(T) \quad (9)$$

where  $F_{m,c}(t)$  is the current fraction of mixture  $m$  in composition  $c$ .

The steady-state module includes provision for a composition search, in which the  $F_{m,c}$  values are varied in specified regions until the system is critical. In such cases, the mixtures whose volume fractions are to be increased are identified by a flag as “fissile” mixtures; others may be identified as “fertile” mixtures. A single search parameter  $x$  (initial value=1.0) is varied such that

$$F_{m,c}^{fissile} = F_{m,c}^{fissile}(0) \cdot x$$

and

$$F_{m,c}^{fertile} = F_{m,c}^{fertile}(0) \cdot \left[ 1 - \frac{\sum_{fissile} F_{m,c}(0)}{\sum_{fertile} F_{m,c}(0)} (x - 1) \right] \quad (10)$$

This procedure preserves the sum of the volume fractions over mixtures in the composition, and the ratio of each fissile (fertile) volume fraction to the remaining fissile (fertile) volume fractions. If the search is carried out in more

than one composition, the ratios of “fissile” volume fractions between compositions is constant, but in general this is not true for “fertile” compositions. Note that the volume fractions entered for mixtures in a composition-search problem must be true volume fractions in order to preserve the total volume of material in the region. Also, the terms “fissile” and “fertile” are purely formal; the actual mixtures varied may represent, for example, control rods and rod followers.

## 2. Group Collapsing

The setup module has provision for group collapsing of the complete cross-section file before the problem begins, using a single weighting spectrum  $\Phi$ . (See Section IX.A.) Using lowercase subscripts  $j$  and  $k$  to indicate fine groups and  $J$  and  $K$  to represent collapsed groups, the various collapsed cross sections are calculated as follows:

capture and fission: 
$$\sigma_{J,i}^x = \frac{1}{\Phi_J} \sum_{j \in J} \sigma_{j,i}^x \Phi_j,$$

where 
$$\Phi_J = \sum_{j \in J} \Phi_j; \quad (11)$$

total nu: 
$$v_{J,i} = \sum_{j \in J} v_j \sigma_{j,i}^f \Phi_j / \sum_{j \in J} \sigma_{j,i}^f \Phi_j \quad (12)$$

transfer: 
$$\sigma_{JK,i} = \frac{1}{\Phi_K} \sum_{j \in J} \sum_{k \in K} \sigma_{jk,i} \Phi_k; \quad (13)$$

transport:

Option 1: 
$$\sigma_J^{tr} = \frac{1}{\Phi_J} \sum_{j \in J} \sigma_{j,i}^{tr} \Phi_j; \quad (14)$$

Option 2: 
$$\sigma_J^{tr} = \Phi_J / \sum_{j \in J} (\Phi_j / \sigma_{j,i}^{tr}); \quad (15)$$

Option 3: 
$$\sigma_{J,i}^{tr} = \frac{1}{\Phi_J} \sum_{j \in J} \left[ 2 \left( \sigma_{J,c}^{tr} / \sigma_{j,c}^{tr} \right)^2 - \sigma_{J,c}^{tr} / \sigma_{j,c}^{tr} \right] \sigma_{j,i}^{tr} \Phi_j, \quad (16)$$

where  $\sigma_{j,c}^{tr}$  is the homogenized transport cross section for a reference composition and  $\sigma_{j,c}^{tr}$  is calculated as in Option 2. The Option 3 procedure was developed by Travelli.<sup>24</sup>

$$\text{Velocity: } v_j = \Phi_j / \sum_{j \in J} (\Phi_j / v_j). \quad (17)$$

The collapsed set is written onto logical unit 02, which may be saved for later use.

### 3. Transverse Bucklings

There are four options for input of the transverse leakage-absorption values. (See Sections VI.A.7, variable KUBUCK, and VI.A.8, variable BUCK(J,M).) The last two options require direct input of buckling values. The first two options require the transverse dimension as input. When the calculation is in slab geometry, the transverse dimension is assumed to be a bare cylinder;  $B^2$  is calculated by

$$B^2 = (2.404826/R)^2,$$

where R is the input value.

When the problem is cylindrical,  $B^2$  is given by

$$B^2 = (3.14159265/H)^2,$$

where H is the input value

### B. Steady-state Module

The purpose of the steady-state algorithm is to compute the initial conditions for the transient. The required initial values are real and adjoint fluxes, precursor densities, power densities, and the associated integral parameters of the quasistatic approximation. The initial system may be either critical with no external neutron source, or subcritical with a source. In the first case, the system may be varied (by changing composition, dimension, or transverse leakage) to achieve criticality, or the critical initial system may be defined as that system in which the true values of neutrons emitted per fission are divided by the  $\lambda$ -eigenvalue of the steady-state equations. The real flux of a critical system may be normalized to a given total reactor power.

A highly simplified fuel-temperature calculation served the purpose of testing the performance of the model in the presence of feedback. The assumption made for the regionwise initial fuel temperature is that the heat-removal rate is equal to the production rate at whatever fuel temperature is input to the problem. This assumption eliminates the need for a steady-state iteration between neutronics and thermal hydraulics to establish consistent initial conditions. The general sequence of operations during the steady-state phase of the calculation is listed in Table III.

TABLE III. Sequence of Steps during Setup and Steady-state Calculations

Operation	Comments
1. Read problem specifications.	Card input
2. (Optional) Generate microscopic cross-section file	Card input
3. Read microscopic-cross section file, and generate mixture cross sections.	User's library file
4. Generate composition cross section; solve for fluxes and eigenvalue	No eigenvalue problem if external source $\neq 0$
5. Test eigenvalue; vary search parameter, and repeat 4 to convergence.	No search if external source $\neq 0$
6. Solve source-free adjoint equation	Weight function for integral kinetics parameters
7. Normalize fluxes and set up initial conditions for dynamic calculation	Completion of preparation for transient calculation

### 1. Steady-state Equations

The multigroup neutron-diffusion and delayed-neutron precursor equations at a point in the system are written

$$\begin{aligned}
 0 = & D_g \nabla^2 \phi_g - \sigma_g^r \phi_g + \sum_{g' < g} \sigma_{gg'} \phi_{g'} + \left( \frac{1}{k} \right) x_g^p \sum_{g'} v_{g'}^p \sigma_{g'g}^f \phi_{g'} \\
 & + \sum_s \lambda_s x_{sg}^d C_s + Q_g \quad (1 \leq g \leq G)
 \end{aligned} \tag{18}$$

and

$$0 = \frac{1}{k} v_s^d \sum_{g'} \sigma_{g'g}^f \phi_{g'} - \lambda_s C_s \quad (1 \leq s \leq m), \tag{19}$$

in which the composition (c) subscript on cross sections is understood and where

$\phi_g$  = neutron flux in energy group  $g$ ,

$D_g$  = diffusion coefficient =  $1/(3\sigma_g^r)$ ,

$\sigma_g^r$  = macroscopic removal cross section

$\sigma_{gg'}$  = macroscopic transfer cross section from group  $g'$  to  $g$  (excluding fission)

$k$  = eigenvalue of homogeneous equation;  $Q_g \neq 0, k = 1$

$x_g^p$  = fraction of prompt fission neutrons emitted into group  $g$

$\nu_{g'}^p$  = number of prompt neutrons produced per fission in group  $g'$

$\sigma_{g'}^f$  = macroscopic fission cross section in group  $g'$

$\lambda_s$  = decay constant of delayed-neutron precursor family  $s$

$x_{sg}^d$  = fraction of delayed neutrons emitted into group  $g$  from decay of precursors in family  $s$

$C_s$  = delayed-neutron precursor concentration in family  $s$

$Q_g$  = external source of neutrons into group  $g$

and

$\nu_s^d$  = number of delayed neutron precursors produced in family  $s$  per fission in any energy group

Several assumptions are implicit in the form of the equations; these were discussed in detail in Section II.

The coefficients  $D_g, \sigma_g^r, \sigma_{gg'}, \nu_{g'}^p, \sigma_{g'}^f$ , and  $\nu_s^d$  are constant over spatial regions within the system, and the Laplacian is approximated on a fine spatial-mesh structure within regions. Flux and current continuity conditions are applied at region interfaces.

The spatial finite-difference treatment is identical to that given in Ref. 21, so that only an outline is given here. The first term on the right-hand side of Eq. 18 is approximated by a three-point difference equation based on a constant-gradient approximation for space interval  $i$  (between points  $i$  and  $i+1$ ):

$$\frac{d\phi}{dr}\Big|_i = \frac{\phi_{i+1} - \phi_i}{\Delta r} \quad (20)$$

where  $\Delta r$  is the difference between points  $i$  and  $i+1$ . As a result of this approximation, the Laplacian at space point  $i$  is written

$$\nabla^2 \phi|_i = \frac{1}{\Delta r^2} \left[ \phi_{i+1} - 2\phi_i + \phi_{i-1} + \frac{(N-1)\Delta r}{2r} \{ \phi_{i+1} - \phi_{i-1} \} \right] \quad (21)$$

where  $N=1,2,3$  for slabs, cylinders and spheres, respectively. This approximation is substituted into Eq.19 to give the difference equation within each spatial region. At interfaces between regions, continuity conditions are applied on the flux and the finite-difference representation of the current. Finite-difference approximations to the boundary conditions  $\phi = 0, d\phi/dr = 0$  and  $\phi + \omega d\phi/dr = 0$  are developed for the inner and outer boundaries of the system. The  $\omega$  values may be calculated by the code or given as input. No provision is made in QX1 for treating inhomogeneous boundary conditions.

The finite-difference equations are solved by using a power-iteration procedure accelerated by a three-term Chebyshev polynomial method identical to that presented in Ref. 10, pp. 85-88, except that in QX1 the acceleration is performed on the fission-source distribution rather than on the group fluxes.

## 2. Criticality Search

If  $Q_g = 0$  for all  $g$  in Eq. 18, one of four quantities of the system-- dimension, fuel composition, transverse leakage, or neutron yield per fission-- may be adjusted until  $k = 1$  in Eq. 18. Search options are given in detail in the input description (Section VI); the basic procedure is to adjust the single parameter  $x$  in the expression  $P_R^n = x^n P_R^0$ , where  $P_R^n$  ( $n=0,1,2,\dots$ ) are successive trials of the quantity being varied in region R and where the set of {R} search regions is selected by the user. The initial value is  $x^0 = 1.0$ ; the second trial,  $x^1$ , is given by

$$x^1 = 2 - k^0 \quad (22)$$

The third trial,  $x^2$ , is obtained by extrapolation from the first two trials  $\{x^0, x^1\}$  and the associated eigenvalues  $\{k^0, k^1\}$ , using the form

$$x = Ae^k \quad (23)$$

Successive search trials  $x^3, x^4, \dots$ , are obtained from the expression

$$x = \frac{a - \frac{b}{k}}{1 - \frac{c}{k}} \quad (24)$$

where the constants a,b and c are determined from the last three pairs of  $\{k^n, x^n\}$ , then the desired value of  $k = 1$  is substituted in the equation.

### 3. Adjoint Solution

Substituting Eq. 19 into Eq. 18, setting  $Q_g = 0$ , and transposing the coefficient matrix leads to the source-free adjoint equations:

$$0 = D_g \nabla^2 \psi_g^* - \sigma_g \psi_g^* + \sum_{g' > g} \sigma_{g'g} \psi_{g'}^* + \frac{1}{k_0} \left( \nu_g^p \sigma_g^f \sum_{g'} x_{g'}^p \psi_{g'}^* + \sum_s \nu_s^d \sigma_g^f \sum_{g'} x_{sg}^d \psi_{g'}^* \right) = 0$$

$$(1 \leq g \leq G) \quad (25)$$

where  $\psi_g^*$  is the adjoint flux which is used to weight the integral parameters in the dynamic equations (see Section III.C) and  $k_0$  is the eigenvalue of the source-free system. If  $Q_g = 0$  for all  $g$  in Eq. 18,  $k_0 = 1$  in Eq. 25. If  $Q_g > 0$  for all  $g$ , a uniformly positive solution of Eq. 18 exists only when  $k_0 < 1$ .

The solution of Eq. 25 is obtained by the same iterative procedure as outlined above, except that the energy-group ordering is reversed to improve the convergence rate.

### 4. Normalization

The model is strictly one-dimensional; that is, no integrations are carried out over transverse dimensions. In slab and cylindrical geometries, the integral quantities therefore are per unit area and per unit height, respectively.

When  $Q_g = 0$  for all  $g$  in Eq. 18, the real flux is normalized to a given total power,  $W$ , by solving for the normalization constant  $A$  in the expression

$$W = \frac{A \int \sum_g \sigma_g^f(\vec{x}) \tilde{\phi}_g(\vec{x}) d\vec{x}}{P} \quad (26)$$

where  $P = 2.91 \times 10^{10}$  is the number of fissions per watt-second, and  $\tilde{\phi}_g(\vec{x})$  is the arbitrarily normalized solution of Eq. 18 with  $Q_g = 0$  for all  $g$ . When any  $Q_g \neq 0$ , the normalization of  $\phi_g(\vec{x})$  is determined by the source magnitude, and the fission power  $W$  is calculated from Eq. 26 with  $A = 1$ .

Normalization of the source-free adjoint solution may be chosen to satisfy one further condition. In QX1, the adjoint normalization constant,  $B$ , is calculated from the equation

$$B \int \sum_g \frac{1}{\nu_g} \tilde{\psi}_g^*(\vec{x}) \phi_g(\vec{x}) d\vec{x} = 1 \quad (27)$$

where  $\tilde{\psi}_g^*(\vec{x})$  is the arbitrarily normalized solution of Eq. 25

### C. Dynamic Module

The solution method used in QX1 can be described as successive approximation of the pair of coupled systems which arise from factorization of the original equation system into a flux-shape function equation on the one hand, and all other members of the system on the other. The general development has been presented elsewhere;<sup>1,4,9</sup> the following equations are given for the sake of completeness in this report. The general sequence of operations during the dynamic phase of the calculation is listed in Table IV. These steps are described in detail below.

TABLE IV. Sequence of Steps During Dynamic Calculation

Operation	Comments
1. Select time step $\Delta t_i^n$ .	The first step is arbitrary; later steps are selected by automatic selector.
2. Extrapolate amplitude function $N(t)$ and shape function $\psi_g(x,t)$ .	In $[N(t)]$ is assumed to be parabolic; $\psi_g(x,t)$ is assumed to be linear.
3. Compute material densities and temperatures at end of interval, and compute coefficients of $N(t)$ equation using extrapolated shape function	Driving-function routine and fuel temperature routines at present. Fuel temperatures are used in $\sigma(T)$ Interpolation
4. Interpolate coefficients of $N(t)$ equation in time interval	Parabola through last three points
5. Solve for $N(t)$ over interval, compare computed value with extrapolated value, and iterate from step 3 if necessary	
6. Update spatial precursor densities	Use extrapolated shape function and computed $N(t)$ in convolution integral
7. Test shape-function recalculation criteria, and either repeat from step 1 or recalculate shape function	
8. Solve for new shape function	
9. Using approximate update coefficients, recalculate $N(t)$ over intervals since last shape calculation and iterate to step 8 if necessary	The criterion for iteration is the value of the flux normalization constant $\gamma^{(n)}$
10. Repeat from step 1	

## 1. Time-dependent Equations

The time-dependent equations for the total flux  $\phi$  and precursor density  $C$  are obtained by modifying Eqs. 18 and 19 to include, respectively, the neutron-density time derivative and precursor time derivative on the left-hand side. Since the initial system either is critical or  $Q_g > 0, k = 1$  in the time-dependent equations. (If  $Q_g = 0$  for all  $g$  and no criticality search is carried out in the static module, all neutron yields are modified appropriately so that, for the new steady-state system,  $k = 1$ .) To simplify, write

$$v = \text{diagonal}\{v_1 \dots v_G\},$$

$$M = \begin{bmatrix} (-D_t \nabla^2 + \sigma_1^r) & 0 & 0 & 0 & 0 \\ \cdot & \cdot & 0 & 0 & 0 \\ (-\sigma_{g1}) & \cdot & \cdot & 0 & 0 \\ \cdot & \cdot & \cdot & \cdot & 0 \\ (-\sigma_{G1}) & \cdot & (-\sigma_{Gg1}) & \cdot & (-D_G \nabla^2 + \sigma_G) \end{bmatrix}$$

( $\nabla^2$  actually is replaced by its finite-difference approximation),

$$F^p = \begin{bmatrix} x_1^p v_1^p \sigma_1^f & \cdot & x_1^p v_G^p \sigma_G^f \\ \cdot & \cdot & \cdot \\ x_G^p v_1^p \sigma_1^f & \cdot & x_G^p v_G^p \sigma_G^f \end{bmatrix}$$

$$F_s^d = \text{row vector } \{v_s^d \sigma_1^f \dots v_s^d \sigma_G^f\},$$

$$x_s^d = \text{column vector } \{x_{s1}^d \dots x_{sG}^d\},$$

$$Q = \text{column vector } \{Q_1 \dots Q_G\}, \quad (28)$$

and

$$\phi = \text{column vector } \{\phi_1 \dots \phi_G\}.$$

The time-dependent equations equivalent to Eqs. 18 and 19 are written

$$v^{-1} \frac{\partial \phi}{\partial t} = (-M + F^p) \phi + \sum_s x_s^d \lambda_s C_s + Q \quad (29)$$

and

$$\frac{\partial C_s}{\partial t} = F_s^d \phi - \lambda_s C_s \quad (1 \leq s \leq m). \quad (30)$$

The coefficients of these equations are functions of  $\phi$  through coupling with feedback phenomena. These may be represented symbolically by

$$\dot{\omega} = P(\phi, \omega). \quad (31)$$

Factorization of  $\phi$  in Eq. 29 into time-dependent amplitude function  $N$  and shape function  $\psi$  is defined by

$$\phi = \psi N \quad (N = 1 \text{ at } t = 0) \quad (32)$$

and

$$\int \sum_g \frac{1}{v_g} \psi_g^*(\bar{x}) \psi_g(\bar{x}, t) d\bar{x} = 1 \quad (t \geq 0), \quad (33)$$

where  $\psi_g^*(\bar{x})$  is the normalized static adjoint solution. Thus  $N$  is a scalar-valued function of time, and  $\psi$  is a vector-valued function of space and time.

The shape-function equation is obtained by substituting Eq. 32 into Eq. 29 and dividing through by  $N$ :

$$v^{-1} \frac{\partial \psi}{\partial t} = \left( -M + F^p - v^{-1} \frac{\dot{N}}{N} \right) \psi + \frac{1}{N} \sum_s x_s^d \lambda_s C_s + \frac{Q}{N}. \quad (34)$$

The spatial precursor equations are integrated formally to obtain

$$C_s(t) = C_s(0) \exp(-\lambda_s t) + \int_0^t [F_s^d \psi] N \exp[-\lambda_s(t-t')] dt' \quad (1 \leq s \leq m). \quad (35)$$

The amplitude function and integrated precursor equations are obtained by taking the inner product of  $\Psi^* = \{\psi_1^* \dots \psi_G^*\}$  with Eq. 29 and  $\Psi^* x_s^d$  with Eq. 30, and carrying out simple rearrangement of terms. The result is

$$\dot{N} = \left( \frac{\rho - \beta}{\Lambda} + \frac{k_0 - 1}{\Lambda k_0} \right) N + \sum_s \lambda_s \eta_s + \frac{Q'}{F\Lambda} \quad (36)$$

and

$$\dot{\eta}_s = \frac{\beta_s}{\Lambda} N - \lambda_s \eta_s \quad (1 \leq s \leq m), \quad (37)$$

where

$$\rho = \frac{1}{F} \left\langle \psi^*, \left[ -M + \frac{1}{k_0} \left( F^p + \sum_s x_s^d F_s^d \right) \right] \psi \right\rangle,$$

$$\beta_s = \frac{1}{F} \left\langle \psi^*, x_s^d F_s^d \psi \right\rangle, \quad \beta = \sum_s \beta_s,$$

$$\Lambda = \frac{1}{F} \left\langle \psi^*, v^{-1} \psi \right\rangle = \frac{1}{F},$$

$k_0$  = eigenvalue of Eq. 25,

$$\eta_s = \frac{1}{F\Lambda} \left\langle \psi^*, X_s^d C_s \right\rangle,$$

$$Q' = \left\langle \psi^*, Q \right\rangle,$$

and

$$F = \left\langle \psi^*, \left[ F^p + \sum_s x_s^d F_s^d \right] \psi \right\rangle. \quad (38)$$

One arbitrary choice is made in developing Eq. 36, namely, that  $\rho = 0$  at  $t = 0$ . The form of the  $\rho$  expression is affected by this choice, and the  $(k_0 - 1) / \Lambda k_0$  term is present because of it. It would be possible to define  $\rho$  with respect to some critical state obtained by adjusting one or more of the coefficients of Eq. 25; however, this critical state usually is undefined.

The choice of the denominator  $F$  is made in order to cancel this quantity in the numerator of the  $(k_0 - 1) / \Lambda k_0$  term. The term  $(k_0 - 1) / k_0$  therefore has the appearance of a “subcritical reactivity” in the initial system when  $Q \neq 0$ .

## 2. Initial Conditions

The initial conditions of the system are defined by Eqs. 18 and 25-27, along with the initial heat-removal rate in the simplified fuel-temperature feedback model (see Section VIII).

One problem arises in computing the  $\rho$  term in Eq. 36. In principle, when  $t = 0$ ,

$$\rho = \frac{1}{F} \left\langle \psi^*, \left[ -M + \frac{1}{k_0} \left( F^p + \sum_s x_s^d F_s^d \right) \right] \psi \right\rangle \equiv 0 \quad (39)$$

by definition of  $\psi^*$  in Eq. 25. This will be true exactly if the form of the approximation to the differential operator used in the inner-product calculation is

the same as that used in the calculation of  $\psi^*$ , and if the iterative solution procedure used in solving Eq. 25 is fully converged.

During coding of QX1, it was felt to be impractical to reproduce the finite-difference coefficients in the inner-product routine. Instead, the usual volume-to-surface integral transformation of the differential term is carried out, and the resulting real and adjoint function gradients are approximated by Eq. 20. As a result, Eq. 39 is not satisfied exactly. The procedure used in QX1 is to compute this residual at  $t=0$  and to subtract it from all  $\rho$  values for  $t \geq 0$ . Thus the discrepancy between the reactivity computed from the finite-difference approximation, and the reactivity calculated by the inner-products algorithm is canceled approximately for  $t > 0$  if the shape function does not change drastically during the excursion. The magnitude of this residual decreases with decreasing mesh spacing as the two approximations to the differential operator approach each other, so that its effect on the solution can easily be evaluated.

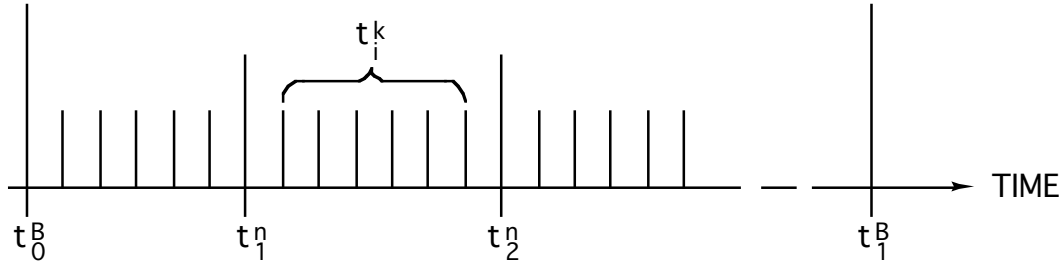
For inhomogeneous problems (subcritical reactor with constant initial external source), a test is carried out to verify convergence of the real flux magnitude. Solution of Eqs. 36 and 37 for steady-state conditions shows that the required condition is

$$1.0 = -\frac{Q'}{F} \cdot \frac{1}{\rho}$$

If this condition is not met within the steady-state source-convergence criterion, the real fluxes are normalized and the steady-state module is reentered to obtain the property normalized solution before the dynamic calculation is started.

### 3. Sequence of Solution

Figure 1 shows the three-level time-step structure of QX1. The system to be solved is represented by Eqs. 31 and 34-37. The approach used is to treat



#### Definitions

$t_i^B$  : Time points at which new shape functions are calculated.

$t_i^n$  : Time points at which coefficients of amplitude-function equations are recalculated, using volume fractions and temperatures determined by driving functions and feedback equations.

$t_i^k$  : Time points used for integration of the amplitude-function equations, Eqs. 36 and 37. Feedback equations may be integrated in any time steps within the range  $t_{i-1}^n$  to  $t_i^n$ .

Figure 1 – Time-step Sequence

Eq. 34, the shape-function equation, as one member of a pair of coupled systems, and Eqs. 35-37 and the entire set of feedback equations as the other member of the pair. The procedure of obtaining an approximate solution is as follows.

Suppose that the state of the system is known up to time  $t_0^B$  (Fig. 1). Let successive iterates of the various parts of the solution be identified with parenthesized superscripts  $(i, j, k, \dots)$  where each superscript identifies a particular level of iteration. Time advance to  $t_1^B$  is initiated by extrapolating the shape function linearly over time points  $t_{-1}^B$  and  $t_0^B$  to provide the first estimate  $\psi^{(j)}, j=1$ , for the shape function in the interval  $[t_0^B, t_1^B]$ . The time point  $t_1^n$  is then determined by the time-step selector (see Section IV.A). The estimated amplitude function  $N^{(j,k)}, j=k=1$ , is then extrapolated from the previous three  $t_i^n$  points including time  $t_0^B$ , using the function

$$1nN^{(j,k)} = a + b(t - t_0^B) + c(t - t_0^B)^2, \quad (t_0^B \leq t \leq t_1^n). \quad (40)$$

This  $N^{(j,k)}$  approximation is used to compute the energy generated over the interval in each reactor region for the fuel-temperature calculation (see Section VIII).

Values of material volume fractions, temperatures, etc., at  $t_1^n$  are calculated from the system driving functions (see Section V) and fuel temperature routine (see Section VIII). The current volume fractions and temperatures then are used to form the composition cross sections required to calculate the coefficients of Eqs. 36 and 37 at  $t_1^n$ . The values of these coefficients in the range  $[t_0^B, t_1^n]$  are approximated by parabolas passing through the last three such time points. The quantities approximated in this way are  $\rho/\Lambda, \beta_s/\Lambda$  and  $Q'/F\Lambda$ .

The next step is the solution of Eqs. 36 and 37 over the interval. The procedure used is the subdomain weighted-residual procedure described in Ref. 26 including automatic time step adjustment. The equations are solved on both a full- and half-interval mesh. In a given  $\Delta t_i^k$  step, the half-interval result is compared with the full-interval result. If the relative discrepancy is greater than a convergence limit, the step length is halved and the interval repeated. If the relative discrepancy is less than 1/10 of the convergence limit, the interval is accepted and the following step length is doubled. Between 1 and  $(2^{18} - 1)$  time intervals  $\Delta t_i^k$  may be taken within each  $[t_0^B, t_1^n]$  step as required to satisfy a convergence criterion on  $N(t)$ . When the solution for  $N(t)$  has been advanced to  $t_1^n$  it is compared with the extrapolated value given by Eq. 40. If the percentage difference is outside a specified limit, the amplitude function solution procedure is repeated over the interval  $[t_0^B, t_1^n]$  using successive values of  $N$  at  $t_1^n$  to form the coefficients of Eq. 40. The iteration is identified as the k-iteration with successive values  $N^{(j,k)}$  and converged result  $N^{(j)}$ .

When  $N^{(j)}$  has been obtained, the spatial precursor equation, Eq. 35 is updated to  $t_1^n$  in the form

$$C_s^{(j)}(t_1^n) = C_s(t_0^B) \exp[-\lambda_s(t_1^n - t_0^B)] + a_s^{(j)} [F_s^d \psi(t_1^n)] + b_s^{(j)} [F_s^d \psi(t_0^B)], \quad (41)$$

where

$$a_s^{(j)} = \frac{1}{t_1^n - t_0^B} \int_{t_0^B}^{t_1^n} \exp[-\lambda_s(t_1^n - t)] (t - t_0^B) N(t) dt$$

and

$$b_s^{(j)} = \frac{1}{t_1^n - t_0^B} \int_{t_0^B}^{t_1^n} \exp[-\lambda_s(t_1^n - t)](t_1^n - t)N(t)dt.$$

These expressions result from the assumption that the delayed-neutron production rate in family  $s$  per unit amplitude function,  $F_s^d \psi$ , is linear in the interval  $[t_0^B, t_1^n]$ . Numerical integration of the  $a_s^{(j)}$  and  $b_s^{(j)}$  terms is carried out on the  $t_i^k$  mesh structure within the interval.

The next operation is testing of the shape recalculation criteria (see Section IV.B). If specified limits on changes since time  $t_0^B$  have not been exceeded, the calculation proceeds to  $t_2^n$  and so on. (The time-step selectors include look-ahead algorithms to predict the next  $t_i^B$  time point.)

When time  $t_i^B$  has been reached (i.e., when one or more of the shape-recalculation criteria are exceeded) an approximate solution  $\psi^{(j)}$  is found for Eq. 34. The equation first is approximated by replacing the left-hand side by the implicit difference term

$$v^{-1} \frac{\partial \psi}{\partial t} \Big|_{t_1^B} \approx \frac{1}{\Delta t^B} v^{-1} [\psi(t_1^B) - \psi(t_0^B)] \quad (42)$$

where  $\Delta t^B = t_1^B - t_0^B$ , resulting in the expression

$$\left\{ v^{-1} \left[ \frac{1}{\Delta t^B} + \left( \frac{N}{N} \right)^{(j)} \right] + M^{(j)} \right\} \psi^{(j+1)} = (F^p)^{(j)} \psi^{(j+1)} + \hat{Q}^{(j)}$$

with

$$\hat{Q}^{(j)} = \frac{1}{N^{(j)}} \left\{ \sum_{s=1}^m x_s^d \lambda_s C_s^{(j)} + Q \right\} + \frac{1}{\Delta t^B} v^{-1} \psi(t_0^B) \quad (43)$$

The  $j$  superscript on elements of Eq. 43 indicates that this element is the result, at time  $t_1^B$ , of a  $j$ th iteration approximation. As a result, there are errors in all  $j$  superscript terms resulting from approximations made in previous iterations.

Generally  $\psi^{(j+1)}$  will not satisfy Eq. 33. When the system approaches prompt critical,  $C_s^{(j)} / N^{(j)}$  becomes very small, and since  $v_g \Delta t^B \gg 1$  for all groups in typical cases, the  $\hat{Q}^{(j)}$  term in Eq. 43 approaches zero. The magnitude of  $\psi^{(j+1)}$  therefore becomes very sensitive to errors in the individual terms, and the equation becomes difficult to solve by iterative inversion. For these reasons, a

normalization factor  $\gamma^{(j,\ell)}$  is introduced inside the inversion iteration ( $\ell$  iterates) in the following way. Equation 43 becomes, during these  $\ell$  iterates,

$$\left\{ v^{-1} \left[ \frac{1}{\Delta t^B} + \left( \frac{\dot{N}}{N} \right)^{(j)} \right] + M^{(j)} \right\} \psi^{(j+1,\ell+1)} = \frac{1}{\gamma^{(j+1,\ell)}} F^B \psi^{(j+1,\ell)} + \hat{Q}^{(j)}$$

where

$$\gamma^{(j+1,\ell)} = \langle \psi^*, v^{-1} \psi^{(j+1,\ell)} \rangle \quad (44)$$

The  $\gamma$ -factor approximation is discussed in the following subsection.

The solution  $\psi^{(j+1)}$ , which is the result of the converged  $\ell$  iterations (these are accelerated by the same three-term Chebyshev procedure as the steady-state problem), could be used together with  $\psi(t_0^B)$  to form linearly interpolated values of  $\psi$  for the  $(j+1)$  iterate over the time interval  $[t_0^B, t_1^B]$ . The same sequence of calculations as described above for the first iteration would be repeated for each  $j$  iteration. This sequence may involve a large amount of calculation in a production version of QX1 in which feedback routines are calculated. Two simplifying approximations are made. First, it is assumed that the first iterate values of volume fractions and temperatures are sufficiently accurate. Second, corrections to the amplitude-function coefficients at points  $t_i^n$  are computed approximately. If  $\alpha = (t - t_0^B) / (t_1^B - t_0^B)$  and (using the  $\rho$  function as an example)  $\rho^{(1)}(t_1^B)$  and  $\rho^{(j)}(t_1^B)$  are the reactivity at  $t_1^B$  as calculated with the first and  $j$ th iteration of  $\psi$ , respectively, then the reactivity for  $j \leq 2$  is corrected by

$$\rho^{(j)}(t_i^n) = \rho^{(1)}(t_i^n) + \alpha \{ \rho^{(j)}(t_1^B) - \rho^{(1)}(t_1^B) \} \quad (45)$$

This approximation is discussed in the next subsection.

Finally, the  $j$  iteration is continued as above until

$$|\gamma^{(j+1)} - 1| < \epsilon \gamma \quad (46)$$

where  $\epsilon \gamma$  is a specified convergence criterion. The iteration is terminated at the end of the  $(j+1)$ st sweep of the amplitude function calculation. During these iterations, only Eqs. 36 and 37 are solved with updated coefficients as given (for example) by Eq. 45. For reasons of economy the spatial precursor equation, Eq. 35, is not included in the  $j$  iteration.

#### 4. Numerical Approximations

The basic approximations are the three-point spatial difference of the Laplacian given by Eq. 21 and the implicit time difference of the shape function, Eq. 42. Several other approximations have been made in order to reduce computation time; the rationale for these approximations is presented here.

The most important approximation from the point of view of economy is the  $\gamma$  factor introduced in Eq. 44. The primary advantage of this technique is that, as  $\hat{Q}^{(j)}$  tends to zero in Eq. 44 (around prompt critical), the  $\ell$  iteration becomes a power-iteration sequence of a homogeneous system, with  $\gamma^{(j+1)}$  as eigenvalue. In a typical fast reactor, the eigenvalue dominance ratio is 0.7 or 0.8, so that acceleration procedures are very efficient. On the other hand, solution of Eq. 43 when  $\hat{Q}^{(j)} \rightarrow 0$  involves estimating an eigenvalue which may be less than 1 by only  $10^{-5}$  or  $10^{-6}$ , in the case of  $v_g \Delta t^B \gg 1$ . This problem could be avoided by reducing  $\Delta t^B$ . However,  $v_g$  is so large that very small time steps would be required and all advantages of flux factorization would be lost. The  $\gamma$ -factor iteration scheme has been found to converge very rapidly in fast-reactor transient calculations;  $|\gamma - 1|$  usually is reduced by an order of magnitude on each  $j$  iteration.

A complete shape function-amplitude function iteration would involve recalculation of all feedback terms and the inner products which are coefficients of the amplitude equations. The first approximation made at this point is to accept the first  $j$ -iterate values of volume fractions and temperatures. This essentially makes the iteration into an open loop. Second, to avoid recalculation of inner products, the approximation represented by Eq. 45 is made. This is based on the following. The basic approximation is that the shape function is linear in the interval  $[t_0^B, t_1^B]$ . Also, the end-point values  $\psi(t_0^B)$  and  $\psi^{(j)}(t_1^B)$  each satisfy Eq. 33. Therefore, at any time in the interval, the current reactivity value (for example) is

$$\rho^{(j)}(t_i^n) = \alpha \rho[\psi^{(j)}(t_1^B)] + (1 - \alpha) \rho[\psi(t_0^B)], \quad (47)$$

where

$$\alpha = (t_i^n - t_0^B) / (t_1^B - t_0^B), \text{ and } \rho[\psi^{(j)}(t_i^B)]$$

Indicates the reactivity at time  $t_i^n$  as computed with a particular shape function.

The difference between  $\rho^{(j)}(t_i^n)$  and  $\rho^{(1)}(t_i^n)$  is

$$\rho^{(j)}(t_i^n) - \rho^{(1)}(t_i^n) = \alpha \left\{ \rho[\psi^{(j)}(t_1^B)] - \rho[\psi^{(1)}(t_1^B)] \right\} \quad (48)$$

The approximation in Eq. 45 relative to the correct expression Eq. 48 is that the difference of reactivities

$$\left\{ \rho[\psi^{(j)}(t_1^B)] - \rho[\psi^{(1)}(t_1^B)] \right\}$$

calculated at time  $t_i^n$  is replaced by the same quantity calculated at time  $t_1^B$ , the end of the interval.

The first iteration solution of the spatial precursor equation, Eq. 41 is accepted. This approximation can be justified by the relatively minor importance of the precursor shape function in determining the flux shape function. As a result of this approximation, the spatial precursor concentrations are never strictly compatible with the integral precursor concentrations as calculated from Eq. 37.

The above approximations can be tested by reduction of time and/or spatial mesh intervals; all of them have been found to be of practical value in reducing the running time of QX1. More importantly, they have been tested in preparation for the multidimensional capability toward which this development is directed.

## 5. External Sources; First-collision Distributions

The external source  $Q$  in Eq.29 may be the sum of two terms. First, a point-dependent total source density with a single emission spectrum, say  $Q_1$ , has the form

$$Q_1 = x_1^{ex} Q^T f(t) \quad (49)$$

where  $x_1^{ex}$  is the normalized emission spectrum,  $Q^T$  is the normalized source density, and  $f(t)$  is a time function entered as one of the system driving functions (see Section V). The steady-state source distribution in Eq. 18 is limited to the form of  $Q_1$ .

The second type of source,  $Q_2$  is a simplified first-collision distribution. Neutrons are presumed to enter the system at the origin, again with a time dependence  $f(t)$ , but with the restriction  $f(0^-) = 0$ . Their energy dependence is given by a second G-dimensional spectrum vector,  $x_2^{ex}$ . In the case of cylindrical and planar geometries, all neutrons are assumed to be omitted in the coordinate direction of the calculation. (This assumption was not considered important, because of the main emphasis on spherical calculations for pulsed-source problems.)

Due to the mesh-point difference scheme in QX1, a source concentrated at the origin cannot be treated exactly. The following scheme was adopted in an attempt to avoid the complications arising from finite source domain kernels. If  $A(R^1)$  is the surface area of a small artificial region surrounding the source, if zero attenuation is assumed from  $r=0$  to  $r=R^1$  and flight time from 0 to  $R^1$  is ignored, the source rate in group  $g$  at the point  $r=R^1$ , time  $t$ , is given by

$$Q_{2,g}(R^1, t) = \left[ \sum_{g'} \frac{(\sigma_{s,gg'} + x_g^p v_g^p, \sigma_{g'}^f) x_{2,g'}^{ex}}{A(R^1)} \right] f(t) \quad (50)$$

Where  $\sigma_{s,gg'}$ , is the scattering cross section from group  $g'$  to group  $g$ .

It is assumed that the source rate is equal to  $Q_{2,g}(R^1, t)$  at all mesh points within the source region. This approximation can be tested by varying the radius  $R^1$ .

Outside the radius  $R^1$ , the source rate into group  $g$  at point  $r$  in the region  $K$  is computed from

$$Q_{2,g}(r, t) = \sum_{g'} \left\{ (\sigma_{s,gg',K} + x_g^p v_{g',K}^p, K \sigma_{g'}^f, K) x_{2,g'}^{ex} \cdot \exp \left[ - \sum_{k=2}^{K-1} \sigma_{g'}^{tr, k} (R^k - R^{k-1}) - \sigma_{g'}^{tr, K} (r - R^{K-1}) \right] f(t') \right\} \frac{1}{A(r')} \quad (51)$$

where  $t' = t - (r - R^1) / v_{g'}$ . Equation 51 ignores delayed-neutron precursors formed in fissions caused by first collisions. This approximation was made purely for simplicity in the coding. Addition of terms to account for these precursors, which would modify Eqs. 35 and 37, is simple in principle.

It has been found from experience with source distributions of the type  $Q_1$  that the finite-difference equations can give erroneous results occur at the same region boundary  $R^k$ . In such cases, it is advisable to place an artificial region on one side or the other of the boundary at which the source discontinuity occurs. The mesh spacing in this region should be chosen so that no discontinuity of mesh spacing occurs at the point of source discontinuity.

#### IV. TIME-STEP SELECTOR

This section describes the various methods used in selecting the reactivity time steps,  $\Delta t_i^n$ , and the shape-function recalculation steps,  $\Delta t_i^B$ . These methods are necessarily approximate and in some cases arbitrary, so that they cannot be considered the “best” methods under all conditions. The objective is to minimize the calculation time for typical fast-reactor safety problems; step-selection routines must be modified to fit the needs of a particular area of study. Flexibility has been provided as much as is feasible by including a number of step-selection criteria which may be adjusted by the code user.

##### A. Reactivity Recalculation Steps

The next time step,  $\Delta t_i^n$ , must be determined, subject to constraints, given the first  $j$  iteration solution for the amplitude function up to the beginning of the step,  $N^{(j)}(t_i^n)$ . (The first time step of the dynamic solution is calculated as a given multiple of the prompt-neutron generation time.) Dropping the  $j$  iteration superscripts for simplicity, the values  $N(t_{i-2}^n)$ ,  $N(t_{i-1}^n)$ , and  $N(t_i^n)$  are substituted into Eq. 40 to obtain coefficients a, b, and c. The extrapolated amplitude change is to be limited so that

$$10^{-1/\varepsilon_n} \leq \frac{N(t_{i+1}^n)}{N(t_i^n)} \leq 10^{1/\varepsilon_n} \quad (52)$$

or otherwise that  $\varepsilon_n$  time steps will be taken for each decade change in the magnitude of the amplitude function (default value = 2.0) Substituting Eq. 40 into Eq. 52 and ignoring the  $(\Delta t_i^n)^2$  term, the time step estimate is given by

$$\Delta t_i^n = \frac{1n10}{\varepsilon_n} |b + 2c\Delta t_{i-1}^n|^{-1} \quad (53)$$

A second time-step estimate on a given maximum-allowable fuel-temperature rise. From values calculated in the previous time interval  $(\Delta t_{i-1}^n)$ , assuming that the temperature rise is proportional to the energy increment, which is in turn proportional to  $\delta(N\Delta t) = N(t_{i-1}^n)\Delta t_{i-1}^n$ , the difference term  $\delta(N\Delta t)/\delta T$  is calculated, where  $\delta T$  is the maximum calculated fuel-temperature rise in interval  $\Delta t_{i-1}^n$ . This slope is used in the current time step in the expression

$$\Delta t_i^n = \frac{\Delta T_{\max}}{N(t_i^n)} \frac{\delta(N\Delta t)}{\delta T} \quad (54)$$

The default value of  $\Delta T_{\max}$  is  $25^\circ K$ .

In addition to Eq. 53 and 54,  $\Delta t_i^n$  is limited to no more than double the previous step, and is subject to the requirement that the shape-recalculation time  $t_i^B$  must coincide with the end point of some  $\Delta t_i^n$  step. Therefore, the step selector also must scan a list of estimated step lengths which are set by the shape-function step selector and by the driving-function data. The minimum estimated value of  $\Delta t_i^n$  step is iterated until the calculated value of  $N(t_{i+1}^n)$  is within a given convergence limit of the previous estimate (k iteration). On each k iteration, the  $\Delta t_i^n$  is recalculated on the basis of the  $N(t)$  of the previous iterate. The new  $\Delta t_i^{n(k)}$  is compared with the one selected on the previous k iterate:

$$\frac{\Delta t_i^{n(k)}}{\Delta t_i^{n(k-1)}} > \varepsilon_t \quad (55)$$

If this condition is satisfied,  $\Delta t_i^{n(k-1)}$  is used for the  $k$ th iteration. If not, the new step  $\Delta t_i^{n(k)}$  is selected. (Default value of  $\varepsilon_t = 0.75$ .)

## B. Shape-function Recalculation Steps

The shape-function criteria are tested at the end of each reactivity recalculation step; their general principle is to limit the change in some parameter between shape recalculations. The parameters that are tested in the present version are the instantaneous inverse period of the amplitude function, the amplitude function, the integrated shape function in each region, the regional integrals of reactivity, the regional integrals of delayed-neutron source rates, and the changes in coolant velocity in each region. Default values have been entered for all convergence limits; one or more of these may be altered in order to test the calculation accuracy and/or to optimize run time. All the convergence limits are reduced by the code when the system is near prompt critical. This has been found useful in fast-reactor calculations, because the predicted energy generation-rate is extremely sensitive to errors in  $(\rho - \beta)$ , whereas only  $\rho$  is sensitive to errors in the shape function.

In addition to the automatic step selectors, shape recalculations may be forced at present time points by use of the driving-function system (see Section V). Also, the current shape-function interval is limited to within a factor of 10 larger than the previous integral.

Referring to Fig. 1, the following descriptions assume that iteration 1 of the  $j$  sequence has been completed up to time  $t_i^n$ . The step selector first tests the criteria at  $t_i^n$  to determine whether a shape function is required and, if not, provides estimates to the reactivity-recalculation step selector of the times at which each criterion will be exceeded.

### 1. Inverse-period Test

At  $t_i^n$ , the value tested is

$$\left| \alpha(t_i^n) - \alpha(t_0^B) \right| \leq \varepsilon_\alpha \quad (56)$$

The default value of  $\varepsilon_\alpha$  is  $10^6$ . The large value ensures that this test will not be exceeded in ordinary LMFBR problems. The test is only useful for problems in which the inverse period may have a strong influence on the shape-function spectrum.

For extrapolation to  $t_i^B$ , the allowable  $\Delta t_i^n$  is estimated by substituting Eq. 40 in Eq. 56 to give

$$\Delta t_i^n = \frac{1}{2c} \left[ \alpha(t_0^B) \pm \varepsilon_\alpha - \alpha(t_i^n) \right] \quad (57)$$

If the coefficient  $c$  is positive,  $\alpha$  is increasing toward the positive limit, so the sign of the  $\varepsilon_\alpha$  term is positive. If  $c$  is negative, the sign is negative.

### 2. Preset Time Steps

This test is based on the time-look-ahead calculation in the driving-function routine. (See Section V.) That routine produces a value of  $t_i^B$  which is the minimum value indicated after scanning all driving functions.

### 3. Shape-function Change Test

If the shape-function integral in region  $R$  at time  $t$  is

$$I_r(t) = \int_R \sum_g \psi(\vec{r}) d\vec{r} \quad (58)$$

the test is given by

$$\left\{ \frac{\text{Max} \left[ \frac{I_R(t_i^n) - I_R(t_0^B)}{I_R(t_i^n)} \right]}{R} - \frac{\text{Min} \left[ \frac{I_R(t_i^n) - I_R(t_0^B)}{I_R(t_i^n)} \right]}{R} \right\} \leq \varepsilon_\psi \quad (59)$$

The default value of  $\varepsilon_\psi$  is 0.02.

The predicted value of  $t_i^B$  is found by linear extrapolation of the quantity in braces to equal the value of  $\varepsilon_\psi$ . For the first interval ( $\Delta t_0^n$ ) following a shape recalculation, the values computed during the last shape interval are used.

#### 4. Delayed-neutron Source Test

This test is identical in operation to Eq. 59 with  $I_R(t)$  replaced by

$$Q_R(t) = \sum_f \lambda_f \int_R C_f(\vec{r}, t) dt \quad (60)$$

and  $\varepsilon_\psi$  replaced by  $\varepsilon_Q$  (default value=1.0).

#### 5. Coolant-velocity Test

This test is unused in the present version of QX1. The form used is given by Eq. 59, with  $I_R(t)$  replaced by  $V_R^C(t)$ , the coolant velocity in region  $R$  at time  $t$ , and  $\varepsilon_\psi$  replaced by  $\varepsilon_V$ . (default value = 1.0).

#### 6. Regionwise-reactivity Test

If the regional reactivity integral is given by

$$\rho_R(t) = \int_R \psi^*(\vec{r}) \left[ -M + \frac{1}{k_0} \left( F^p + \sum_S x_s^d F_s^d \right) \right] \psi(\vec{r}) d\vec{r} \quad (61)$$

the test is

$$\left\{ \underset{R}{Max} [\rho_R(t_i^n) - \rho_R(t_0^B)] - \underset{R}{Min} [\rho_R(t_i^n) - \rho_R(t_0^B)] \right\} \leq \varepsilon_\rho \quad (62)$$

Equation 61 is simplified by omission of the internal interface leakage terms. The default value  $\varepsilon_\rho$  is  $0.25\beta$ , or 0.001 in problems with no delayed neutrons.

#### 7. Amplitude-function Test

Equation 52 is applied over the shape-function interval, with  $N(t_0^B)$  replacing  $N(t_i^n)$  and  $\varepsilon_B$  (default value = 1.0) replacing  $\varepsilon_N$ . The predicted  $t_i^B$  value is found by substituting Eq. 40 into resulting equation and rearranging to give

$$\Delta t_i^n = \frac{1n10}{\varepsilon_B} - \left| 1n \frac{N(t_i^n)}{N(t_0^B)} \right| \cdot |b + 2c\Delta t_{i-1}^n|^{-1} \quad (63)$$

### 8. Tightening Convergence near Prompt Critical

The epsilon values in tests 1 and 3-7 are reduced by the factor

$$f = 1.0 - (1.0 - \varepsilon_f) \exp \left[ -\frac{1}{2} \left( \frac{\rho - \beta}{\beta \sigma} \right)^2 \right] \quad (64)$$

Where  $\varepsilon_f$  is an adjustable minimum value (default value = 0.1,  $0 < \varepsilon_f \leq 1.0$ ) and  $\sigma = 0.1\sqrt{2 \ln 2}$ , so that the exponential term is 0.5 when  $|\rho - \beta| = 0.1\beta$ .

This procedure allows tight convergence around  $\rho = \beta$  without unnecessarily decreasing shape function intervals in other ranges of reactivity.

## V. DRIVING FUNCTIONS

The driving-function system simulates two types of physical changes: namely, initiating mechanisms such as control-rod movement, and response mechanisms such as control-rod movement initiated by period signal. In addition, changes in internal quantities due to internal conditions can be simulated, such as coolant-density changes initiated by high fuel temperatures. Finally, the system includes fixed time-step controls, conditional tests for turning off other driving functions, and external neutron-source modifiers. The code input consists of a series of separate driving functions (up to 100 members), which may or may not be related to one another. These functions are processed sequentially at each  $t_i^n$  point. Each driving function has five distinct components; these are discussed separately in Sections A-E.

### A. Triggering

Triggering refers to the testing of specified conditions for initiation of changes in some parameters. Once a trigger test has been met, the given modifier (see Section E below) operates on its specified parameter with a fixed time base, either until its time sequence is exhausted or until it is terminated by a trigger from another function.

The conditions that may be tested (input parameter KOP) are reactor time, fuel temperature, volume fraction, power in a given region, or the instantaneous inverse period of the amplitude function. Each may be tested for the condition of "greater than" or "less than" the given trigger value (input parameters KTRIG and VALTR). The initiation time from which the driving function begins is taken as the  $t_i^n$  point at which the trigger value is exceeded. No interpolation is done to find the time within the previous interval at which the trigger was first exceeded.

Excepting the time and inverse-period tests, all others require a region specification (input parameter KUEREG). The fuel-temperature and volume-fraction tests require a mixture specification (input parameter KUEMAT).

The second type of trigger operation is one in which some other driving function (identified by input parameter NMI) is terminated by the trigger test. The system parameter which was being modified by that function is left at its current value; thus, if the terminating function appears before the terminated function in the test sequence, the appropriate value remains equal to that calculated at  $t_{i-1}^n$ ; otherwise, it remains equal to that calculated at  $t_i^n$ . This trigger option can be used to force a shape-function recalculation at a particular time. The driving function to be terminated may be inactive; that is, NMI need not be a function actually specified in the input.

## B. Mixture Modifiers

One of three parameters of a given mixture (identified by the pair of input parameters MODMAT and MODREG) may be modified: namely, volume fraction, temperature, or velocity. (Velocity modification is irrelevant in Edition 5 of QX1.) The parameter to be modified is identified by parameter MOD.

In operation, the ratio of the current value of the modifier,  $X(t_i^n - t_0)$ , to the previous value,  $X(t_{i-1}^n - t_0)$ , multiplies the parameter  $P$ , such that

$$P(t_i^n) = P(t_{i-1}^n) \cdot \frac{X(t_i^n - t_0)}{X(t_{i-1}^n - t_0)} \quad (65)$$

The time  $t_0$  is the initiation time of the driving function (the time at which the trigger test was first passed). More than one driving function may modify the parameter at  $t_i^n$ , in such a case,  $P(t_{i-1}^n)$  would be multiplied by several parameter ratios to give  $P(t_i^n)$ . Note that the initial value of  $X$  is presumed to be unity, so that if the modifier data begins with a value other than 1,  $P$  will undergo a ramp change in the interval  $\Delta t_i^n$  with magnitude  $[X(t_i^n) - 1]$ . Step functions may be approximated in this way by forcing the interval  $\Delta t_i^n$  to be small. In any case, the initial value of the modifier data must be nonzero.

A driving function is turned off either by a trigger from another driving function or when the time range of the modifier is exceeded. In both cases, the last calculated value of the parameter is left unchanged on termination.

## C. Shape-function Step Controller

This driving function forces shape-function recalculation steps at fixed time intervals (input parameter DTMI), beginning at a specified time (input parameter VALTR). The only valid trigger test is time (input parameter KOP=1).

## D. Source Modifiers

Two types of source-modification functions are available. First, the overall magnitude of the external sources  $Q_1$  (Eq. 49) can be modified by a time-dependent but shape-independent multiplier,  $f(t)$ . The modification operates in the same way as is indicated in Eq. 65 for the mixture parameters.

The second type of source modifier is the pulse-intensity function for the first-collision source  $Q_2$ , described in Section III.C.5. This is the only type of driving function in which the initial value of the modifier data can be zero.

### E. Modifier Data

One of two forms of modifier data may be given. The first is a number (input parameter NMI) of discrete values on a fixed time-interval mesh (input parameter DTMI). The first value is referenced to the initiation time of the driving function. If the current time ( $t_i^n$ ) lies between the first and second discrete values, the function is interpolated linearly to  $t_i^n$ , otherwise, a parabola is passed through the three data points whose central value is the nearest point less than time  $t_i^n$ .

The second type of modifier is one of two analytic functions, given by

$$X(t) = 1.0 + A \sin[2\pi B(t - t_0)] \quad (66)$$

or

$$X(t) = A + B e^{C(t-t_0)} \quad (67)$$

The constants  $A, B$  and  $C$  are entered in input;  $t_0$  is the trigger time. The constants must satisfy the usual restriction to nonzero  $X(t)$ ; thus,  $A$  in Eq. 66 and  $B/A$  in Eq. 67 must be less than 1. Other obvious limits must apply to Eq. 67, depending on the signs and magnitudes of  $A, B$  and  $C$ .

### F. Time Look-ahead

The reactivity recalculation time  $t_i^n$  must be determined before the driving function are tested. As a result, a look-ahead scan is made at each  $t_i^n$  point to determine the next smallest time at which (1) a time-triggered driving function is to be turned on, (2) any driving function is to be turned off, or (3) a step-controller driving function indicated the next shape recalculation. No scan is made for driving functions to be initiated by other than a time trigger, since the triggering time point is not well determined. The minimum time of all predicted values is passed to the reactivity-recalculation-step selector (see Section IV.A) at the initiation of the  $\Delta t_{i+1}^n$  step calculation.

## VI. INPUT PREPARATION

### A. Input-card Formats and Data Descriptions

The input consists of cross sections and problem data. The cross sections may be input from cards, XLIBIT binary tape (CDC-3600 version only), or the normal QX1 library file. (The delayed-neutron-precursor data are entered on cards with each problem, along with the problem specifications.) Instructions for preparing the QX1 library file are given in Section IX.A. The data deck structure is listed below.

1. Title card.
2. Parameter and control card.
3. Delayed-neutron precursor data.
4. Isotope-to-mixture specifications.
5. Cross-section file preparation cards (optional; see Section IX.A).
6. Mixture-to-composition specifications.
7. Fixed-point relative-addressed data.
8. Floating-point relative-addressed data.
9. Driving-function specifications.
10. Feedback data (optional).
11. Problem end card.

1. Title Card  
One card, 80-column Hollerith.
2. Parameter and Control Card

FORTRAN		
<u>Format</u>	<u>Name (Dimension)</u>	<u>Description</u>
A5	CNORM	Cross-section file name
IX		Blank
I3	NTAPE	Cross-section options 0: XLIBIT file (LUN01) 1: QX1 library file (LUN02) 2: Card input (see Section IX.A)
I3	NOM	Number of mixtures in the problem (maximum 16, 8 each of temperature-independent and temperature-dependent mixtures)
I3	NOC	Number of compositions (maximum 20)
I3	NOR	Number of spatial regions (maximum 20)

I3	NOG	Number of energy groups (maximum 30)
I3	NOF	Number of delayed-neutron families (maximum 6)
4E12.5	TBASE(4)	Four reference temperatures of temperature-dependent isotopes on the cross-section tape, entered in order of increasing temperature; each of these must agree with the corresponding values for all isotopes which are to be temperature-dependent.

### 3. Delayed-neutron Precursor Data

These data are entered only if the number of delayed-neutron families entered above is greater than zero.

Enter six sets of delayed-neutron data. The set number appropriate to fission of a particular isotope is specified in the Mixture Data (see Section A.4).

Each set contains NOF families.

Card Type	Format	FORTRAN Name (Dimensions)	Description
a	6E12.5	YTOT(6)	Total yield (neutrons/fission) for each of six delayed data sets
b	6E12.5	YFRAC(6,6)	Fractional yield into each of NOF delayed families for the first delayed data set
Repeat card b for each of the six delayed data sets.			
c	6E12.5	DECAY(6)	Decay constants for each of NOF delayed families
d	6E12.5	CHID(30,6)	Fraction of delayed precursors in each of NOF delayed families that emit neutrons into the first energy group

Repeat card d for each energy group.

#### 4. Isotope-to-Mixture Specifications

Cross-section mixing procedures are described in Section III.C.1.

<u>Card Type</u>	<u>Format</u>	<u>Description</u>
a	6X	May be used to number mixtures (not read)
	I6	Number of isotopes in this mixture (maximum 20)
	A4	Mixture classification flag; one of six mnemonics:  FISS: high-reactivity fuel fraction  FERT: low-reactivity fuel fraction  COOL: coolant  CLAD: fuel-pin cladding  CONT: control assembly  STRC: subassembly structure independent of pin cladding
	7A8	Mixture identification
b	I3	For fissionable isotopes, the delayed-neutron data-set number appropriate to the isotope; the set number refers to the position of the entry on card type a of the delayed-neutron precursor data.
	3X	Blank
	A5	Atom density of the isotope in the mixture

The above five fields are repeated, three sets on a card, up to the number of isotopes in the mixture as given on card type a.

Repeat cards types a and b up to the number of mixtures as given on the parameter card (see 2 above).

Each mixture is constructed separately, and the isotopic cross-sections are not retained. Each mixture may appear in one or more compositions (see below); it may at a given time have a different temperature in each composition in which it appears.

5. Cross-section File Preparation Cards (Optional; see Section IX.A).

The routine that reads the cross-section cards prepares a QX1 library file. This file may be saved for later use.

6. Mixture-to-Composition Specifications

Card

<u>Type</u>	<u>Format</u>	<u>Description</u>
a	6X	May be used to number compositions (not interpreted)
	I6	Number of mixtures in the composition (maximum 16; 8 temperature-dependent, 8 temperature-independent)
	7A8,A4	Composition identification
b	I6	Mixture number
	I6	Composition search flag -1: fissile mixture 0: neutral mixture +1: fertile mixture
	E12.5	Volume fraction of the mixture in the composition
	E12.5	Initial temperature of the mixture in this composition

This set of four fields is repeated, one per card, up to the number of mixtures in the composition as given on card type a.

(If the initial static system is to be made critical by changing compositions, all mixtures with  $-1$  search flags will be varied in fixed proportions to one another. If there are any mixtures with  $+1$  search flags, these will be varied inversely so that total fissile plus fertile volume fraction remains constant. See Section III.A.1 for a detailed description of the composition search. Composition search problems must declare at least one "fissile" mixture.)

Card types a and b are repeated up to the number of compositions in the problem as given on the parameter card (see Section A.2). Each composition specified here may appear in any number of spatial regions. Initial temperatures and volume fractions of mixtures in such compositions will be the same; however, they may be varied independently as the problem proceeds.

## 7. Fixed-point Relative-addressed Data

An individual data word is identified by its relative address in the input storage array. The address of the first data word to appear on a particular card is entered on that card. Subsequent data words on that card are stored in sequentially-increasing-number addresses. If no entry is made for a given variable, that address will contain zero.

<u>Format</u>	<u>Description</u>
I2	Number of data words on the card
I2	Blank; more fixed-point data cards will follow
I2	Nonzero; this is the last fixed-point data card
I8	Relative address of the first data word on the card
I0I6	Data words

The following list describes the function of each fixed-point data word.

<u>Relative Address</u>	<u>FORTRAN Name (Dimension)</u>	<u>Description</u>
1	MAKE	Geometry flag: 1 for slab; 2 for cylinder; 3 for sphere.
2	KIND	Search flag: 0 for no search; 1 for dimension search (reactor size not fixed); 2 for composition search; 3 for dimension search (reactor size fixed); 4 for buckling search.
3	NOKREG	Number of search regions. See KREGS below
4	KONIN	Inner boundary condition: 0 for zero gradient; 1 for zero flux; 2 for logarithmic derivative with extrapolation length input (see OMEGI below); 4 for logarithmic derivative with extrapolation length calculated by the code. <sup>21</sup>
5	KONOUT	Outer boundary condition: 0 for zero flux; 1 for zero gradient; 2 for logarithmic derivative with extrapolation length input (see OMEGO below); 4 for logarithmic derivative

with extrapolation length calculated by the code.<sup>21</sup>

6	KUBUCK	Buckling flag: 0 for constant height or radius input; 1 for region-dependent height or radius input; 2 for group-dependent buckling input; 3 for region-and group-dependent buckling input (see Section III.A.3).
7	KUSOR	Source flag: 0 for fission-source guess input by region; 1 for fission-source guess by point; 2 for fission source by region plus pointwise external source; 3 for fission source by point plus external sources. A value greater than 3 identifies a pulse problem with first collision distribution (see Section III.C.5). Set KUSOR equal to 3 plus the driving function number in which the time shape of the pulse is specified.
8	MAXIN	Flux-iteration limit. (Default value = 100)
9	MAXOUT	Search-iteration limit. (Default value = 10)
10	KEND	Final time flag. If 0, the problem will end when $t = \text{FINT}$ . If 1, the problem will end when $t = \text{XX}$ , where $\text{XX} = \text{AMPLIM}$ and/or $\text{XX} = \text{ROLIM}$ . FINT, AMPLIM, and ROLIM are entered in the floating-point relative-addressed data.
11	KUDYS	Shape-function time-derivative flag: 0 for quasistatic model; 1 for factorized model (derivative included); 2 for factorized model with shape-function extrapolation. Options 0 and 1 were used only for model testing; option 2 is recommended.
12	NUMI	The number of driving functions to be entered. (See 9 below.)
13	NEAT	Feedback flag. Set $\neq 0$ to call adiabatic fuel temperature routine. (See Section VI.A.10.)
14	KUIP	Input-print flag: 0 for normal input print; 1 for adding initial cross-section print; 2

		for adding final cross-section prints; 3 for adding both of the above; 4 for all of the above, plus the cross-section print at shape-recalculation steps.
15	KUOP	Output print flag. If 0, print the shape function at each step; if 1, print the shape function only at $t = 0$ and $t = \text{final time}$ ; if 2, print the shape function and precursors at each time step.
16	KUAP	Adjoint flag. If 1, do not print the adjoint shape function; if 0, print the adjoint shape function.
17	KUMP	Composition print flag. If 1, print the mixture-dependent composition data at each reactivity time step; if 0, do not print.
18	KUCHEB	Shape-function iteration data print flag. If 1 print the iteration data; if 0, do not print.
19	KUDUMPT	Dump flag: 0 for no dump; 1 for point-kinetics dump; 2 for shape dump; 3 for both point-kinetics and shape dump. Logical unit 3 is saved if $KUDUMPT > 0$ . (See Section VII for formats.)
20	KUWIG	WIGLE punch flag. If 1, punch the starting points for the WIGLE code (two-group problem only). If 0, do not punch.
21	KUPK	Set equal to 1 to run point kinetics.
22	JAM(70)	Dummy fixed-point container array. Do not enter data in these locations.
92	NINT(20)	Number of mesh intervals in each region.
112	MIR(20)	The composition number for each region.
132	KREGS(20)	NOKREG region numbers, in which the search is to be carried out. These are entered in order of increasing region number, beginning with the first search region.

NOTE: The last fixed-point data card must have a nonzero entry in columns 3-4.

### 8. Floating-point Relative-addressed Data

The relative-addressing methods here are the same as those used for the fixed-point data. The data words are identified by their relative address. The data format is 5E12.5. The first three fields on a card are identical to those of the previous section.

<u>Relative Address</u>	<u>FORTRAN Name (Dimension)</u>	<u>Description</u>
1	EPSIN	Flux convergence criterion for shape solution. (Suggested value = $10^{-5}$ .)
2	EPSOUT	Search convergence criterion for static solution. (Suggested value = $10^{-5}$ .)
3	DESK	Search to eigenvalue DESK. (Default value = 1.0)
4	RZERO	Radius at the inner boundary.
5	POW	Desired power in watts. (Default value = 1 watt.)
6	TMULT	First time-step multiplier. The initial time step will be of length TMULT times the lifetime. (Default value = 1.)
7	FINT	Real time when the calculation is to end (sec).
8	ROLIM	Final reactivity value if KEND = 1. Calculation ends when $\rho(t_f) = \text{ROLIM}$ .
9	AMPLIM	Final amplitude value (if KEND = 1). Calculation ends when $N(t_f) = \text{AMPLIM}$ .
		Note: On output, any of the above three conditions is identified as Test 10.
10	DUMPT	Dump interval. If KUDUMP = 1 or 3, the point-kinetics dump is given at all shape-function steps, plus at times equal to multiple of

		DUMPT, up to the next shape-function time.
11	CRAM(300)	Dummy floating-point container array. Do not enter data in these locations.
311	ROUT(20)	Outer radius of each region.
331	OMEGI(30)	Group-dependent inner boundary extrapolation lengths if KONIN = 2(cm). Extrapolation-length values must be negative.
361	OMEGO(30)	Group-dependent outer boundary extrapolation lengths if KONOUT = 2(cm). Extrapolation-length values must be positive.
391	BUCK(30,20)	Group- and region-dependent buckling values. On input: For KUBUCK = 0, enter one value--the extrapolation height (cylinder) or radius (slab)--from which the buckling is calculated as $B^2 = (\pi / H)^2$ or $[(j_0 / R)]^2$ and distributed over groups and regions. For KUBUCK = 1, enter NOR values, and $B^2$ is calculated and distributed over groups. For KUBUCK = 2, enter NOG buckling values directly, these values being distributed over regions. For KUBUCK = 3, enter NOG x NOR buckling values directly, the input order being NOG values, in increasing region numbers. These values are entered directly into the two-dimensional array, so that the relative address for group $J$ , region $I$ , is given by $A = 391 + (J - 1) + 30(I - 1)$
991	FISOR(150)	Point-dependent starting fission source. On input: For KUSOR = 0 or 2, enter NOR values (if 0, the code assumes a source of 1), region. For KUSOR = 1 or 3, enter the pointwise values, with the inner boundary values entered into FISORB.
1141	FISORB(19)	Boundary values of the starting fission source. If KUSOR = 0 or 2, this array is filled by the code. If KUSOR = 1 or 3, enter the inner boundary values for regions 2 through NOR.

Note: If KUSOR = 1 or 3, FISOR(1) is the value at the innermost mesh point; FISORB(1) is the value on the right-hand side of the mesh point at the inner boundary of region 2. (The fission source is double-valued at boundaries, because of material discontinuities.)

1160	ALPHA	Current inverse period $\alpha(t)$ ; entered only if a static k search with a nonzero alpha is desired. Otherwise, ALPHA is zeroed by the code.
1161	EXSOR(150)	Point dependent external sources; entered if KUSOR = 2,3. In this case, enter the pointwise values, with the inner boundary values entered in EXSORB.
1311	EXSORB(19)	Boundary values of the external sources. If KUSOR > 1, enter the inner boundary values for regions 2 through NOR.
1330	CHIEX(30)	Group-dependent external-source energy spectrum. Entered only if KUSOR > 1.
1440	EPS(20)	Time-step-control convergence criteria. Thirteen criteria are in use; each is preloaded with a default value as indicated below. These defaults have been selected to give fairly tight convergence in a broad range of problems. However, each case must be examined separately. The individual entries are listed in Table V; the tests are described in Section IV.B.

TABLE V. Time-step Convergence Criteria

<u>a. Reactivity-recalculation Tests</u>			
<u>Reactivity Test No.</u>	<u>Relative Address</u>	<u>Default Value</u>	<u>Description</u>
1	1440	2.0	Amplitude function change (number of steps per decade) $\varepsilon_n$ , Eq. 52.

2	1451	25.0	Maximum temperature change (°K) in any region $\Delta T_{\max}$ , Eq. 54.
3	N/A	N/A	Step length not more than double previous full step.

b. Shape-recalculation Tests

<u>Shape Test No.</u>	<u>Relative Address</u>	<u>Default Value</u>	<u>Description</u>
1	1444	$1.0 \times 10^6$	Inverse period ( $\text{sec}^{-1}$ ) $\epsilon_{\alpha}$ , Eq.56.
2	N/A	N/A	Driving function control
3	1445	0.02	Region- and energy-integrated shape-function relative change $\epsilon_{\psi}$ , Eq.59.
4	1446	1.0	Regional delayed-neutron source relative change $\epsilon_{\rho}$ , Eq.60.
5	1447	1.0	Coolant-velocity relative change (inoperative)
6	1452	0.25	Regional reactivity change $\epsilon_{\rho}$ , Eq.62.
7	1450	1.0	Amplitude function change (number of steps per decade) $\epsilon_B$ , Eq.63.
8	N/A	N/A	Shape interval is limited to 10 times previous interval.
10	N/A	N/A	Final time indicator.
N/A	1449	0.1	Minimum value of reduction in other shape test limits at prompt critical $\epsilon_B$ , Eq.64.

c. Iteration Tests

<u>Iteration Level</u>	<u>Relative Address</u>	<u>Default Value</u>	<u>Description</u>
Amplitude	1441	0.75	Step-acceptance test on k iteration. Minimum Value of current estimate at which previous Estimate is accepted $\epsilon_t$ , Eq.55
Amplitude	1442	0.1	Relative error limit of calculated versus extrapolated amplitude function on k iteration.

Amplitude	1443	0.000001	Interval-acceptance test in amplitude-equation Integration.
Shape	1448	0.001	Limit on absolute error in jth iteration $\gamma$ parameter $\varepsilon_\gamma$ , Eq.46.

---

<u>Relative Address</u>	<u>FORTRAN Name (Dimension)</u>	<u>Description</u>
1460	VEL(30)*	Group velocities (cm/sec).
1490	CHIP(30)*	Prompt-neutron-emission spectrum.
1520	SORCHI(30)	The emission spectrum of the neutron pulse for first-collision source calculation.
1550	SIGS(331, 16)*	Scattering matrices of mixtures.
6846	SIGC(30, 16)*	“Capture” cross sections of mixtures (see Eq. 6).
7326	SIGT(30, 16)*	Transport cross sections of mixtures.
7806	SIGF(30, 8)*	Fission cross sections of mixtures.
8046	SIGN(30, 8)*	Prompt-source ( $v^P \sigma_f$ ) cross sections of mixtures.
8286	DOPCO(30, 8, 6)*	Doppler-interpolation coefficients of mixtures.

Note: The last floating-point data card must have a nonzero entry in columns 3-4.

### 9. Driving-function Specifications

See Section V for a discussion of the driving functions.

<u>Card Type</u>	<u>Format</u>	<u>FORTRAN Name (Dimension)</u>	<u>Description</u>
a	I3	MODMAT	Mixture number } to be modified }

I3	MODREG	Region number
I3	KUEMAT	Mixture number
I3	KUEREG	Region number
		} which is to initiate the change
I3	MOD	Function type.
		a. Mixture fraction
		1: Volume fraction
		2: Temperature
		3: Coolant velocity
		4: Turn off driving function number NMI
		b. Shape-step controller
		5: Fixed shape-function time interval
		c. Source modifier
		6: Magnitude of external source $Q_1$
		7: Magnitude of pulsed source $Q_2$
I3	KOP	Trigger logic
		1: "Less than or equal to"
		2: "Greater than or equal to"
I3	KTRIG	Trigger test type
		1: Time
		2: Temperature
		3: Volume fraction
		4: Power
		5: Instantaneous inverse period
I3	NMI	If MOD = 4, the number of the driving function to be turned off; otherwise, type of modifier data.
		When MOD $\neq$ 4, and NMI equals:
		0, card type b contains analytic function coefficients.
		>0, card type b contains NMI tabular values.
E12.5	VALTR(100)	Trigger value.

E12.5	DTMI		Time interval between modifier data points as given on following card type, or shape-function time interval if MOD = 5. Not used if NMI = 0.
b(option 1)	6E12.5		Present when MOD ≠ 4 or 5 and NMI > 0. Tabular points of modifier data.
(option 2)			Present when MOD ≠ 4 or 5 and NMI = 0.
	A3	ANUMN	Hollerith characters 'SIN' or 'EXP" (see Eqs. 66 and 67).
	E12.5		Coefficient A.
	E12.5		Coefficient B.
	E12.5		Coefficient C if ANUMN contains EXP; otherwise, unused.

\* These data normally are read from the cross-section file. They may be overwritten here.

### 10. Feedback Data

This section is a skeletal remainder of a simple heat-transfer routine which was present in the development version of QX1. Only the fourth and sixth entries (REFAC and FUCAP) are relevant to the adiabatic fuel-temperature routine which is used currently. (See Section VIII.) All eight card types must be entered for each region, but only REFAC and FUCAP need be nonzero.

<u>Card Type</u>	<u>Format</u>	<u>FORTRAN Name (Dimension)</u>	<u>Description</u>
a	6E12,5	COV(20)	Regionwise coolant velocities ( $v_c$ ) in cm/sec.
b	6E12.5	COT(20)	Coolant inlet temperature in °K.
c	6E12.5	HETCON(20)	Regionwise fuel-coolant heat-transfer time constants in sec <sup>-1</sup> .
d	6E12.5	REFAC(20)	Regionwise radial reduction factors for effective-temperature

			calculations.
e	6E12.5	COCAP(20)	The regionwise coolant heat capacities,  $\frac{1}{\rho c}, \text{in } \frac{\text{cm}^3 \times \text{°K}}{\text{W} \times \text{sec}}$
f	6E12.5	FUCAP(20)	The regionwise fuel heat capacities  $\frac{1}{\rho c}, \text{in } \frac{\text{cm}^3 \times \text{°K}}{\text{W} \times \text{sec}}$
g	6E12.5	PICT(20)	The regionwise pin conduction terms, equal to $a^2/8K$ in $\text{cm}^3 \times \text{°K/W}$ .
h	6E12.5	PIST(20)	The regionwise pin surface terms, equal to $a^2/2H$ in $\text{cm}^3 \times \text{°K/W}$ .

### 11. Problem End Card

One card, with the Hollerith name PROBEND in columns 1-7.

### B. Sample Problems

The very large range of possible data configurations makes it impracticable to present a balanced set of sample problems. The two problems discussed below provide illustrations of the card layout produced by the input specifications. Problem 1 is the test problem distributed along with the QX1 code package.

The data entry identifying each characteristic of the problem is given in parentheses immediately following the first mention of the characteristic.

#### 1. Test Problem 1 (see Table VI)

The notable features of this deck are the cross-section file preparation block (NTAPE = 2 on the parameter card) and the feedback block (NEAT ≠ 0, address 13 in fixed-point data). The code will read BCD card images from logical unit 01 (NTP = 1 on card SIG PREP), collapse cross sections from the original 26-group structure to nine groups (parameters NGPS and NCOL on card ANO), carry out a composition search (KIND = 2, address 2 in fixed-point data) to establish a critical system, and run a transient up to 0.075 sec (FINT = 7, address 7 in floating-point data). The transient will be initiated by removal of sodium (mixture 10) from regions 1 and 2. (See cards marked DRIVE 1 and DRIVE 2.)







15	0.0031590	4	0.0002320	5	0.0004412						
5	8CONT	CONTROL ZONE				MIX					5
12	0.011320	15	0.003254	16	0.0015525						
2	0.010601	3	0.057527	8	0.004126						
4	0.0002389	5	0.00001050								
6	ICOOL	INNER CORE ZONE, SODIUM				MIX					6
8	0.022										
7	6STRC	REFLECTOR				MIX					7
21	0.00	30	0.0087204	34	0.0480720						
33	0.0024320	22	0.000	26	0.0067544						
8	4STRC	RADIAL SHIELD				MIX					8
26	0.006754	30	0.039849	33	0.011258						
34	0.005372										
1	1	EJECTED SUBASSEMBLIES FOR ROD DROP SIMULATION				COMP					1
1	-1	1.0	300.0								
2	2	INNER CORE ZONE, COMP. SEARCH PORTIONS				COMP					2
3	-1	0.52580324	300.0								
6	+1	0.47419676	300.								
3	2	OUTER CORE ZONE OF FTR 3				COMP					3
2	-1	0.3444	300.0								
4	0	1.0	300.0								
4	1	FTR3 CONTROL RING				COMP					4
5	0	1.0	300.0								
5	1	RADIAL REFLECTOR				COMP					5
7	0	1.0	300.0								
6	1	RADIAL SHIELD				COMP					6
8	0	1.0	300.0								
3	1	2	0	2		FIXED					PT
1	7	2									
1	8	300									
2	11	2	5								
1	17	1									
1	19	3									
8	92	2	3	2	11	12	2	12	6		
8	112	1	2	1	2	3	4	5	6		
2	1	132	2	4						FIXED	PT
2	1	1.0	E-05	1.0	E-05					FLOAT	PT
2	6	1000.0	0.6								
1	7	30.0									
1	10	0.03									
5	311	3.1199	9.3597	11.24896	37.575	60.1561					
5	316	62.131198	85.1146	97.0857							
1	391	134.755650									
5	116113.52454331213.52454331213.524543312				13.287	13.287					
5	1166	13.287	13.52454331213.524543312		13.287	13.287					
5	1171	13.287	13.287	13.287	13.287	13.287					
5	1176	13.287	13.287	13.287	13.287	13.287					
5	118028.19223254628.19223254628.19223254628.19223254628.192232546										
5	118528.19223254628.19223254628.19223254628.19223254628.192232546										
2	119028.19223254628.192232546										
4	1311	13.287	13.524543312	13.287	28.192232546						
5	1330	3.24802E-02	1.21769E-01	2.10943E-01	2.22961E-01	1.72783E-01					
5	1335	1.10467E-01	6.27520E-02	3.31622E-02	1.67701E-02	8.25646E-03					
5	1340	3.99931E-03	1.91817E-03	9.14497E-04	4.34408E-04	2.05900E-04					
5	1345	9.74611E-05	4.60950E-05	2.17903E-05	1.02977E-05	4.86567E-06					
5	1350	2.29877E-06	1.08587E-06	5.13010E-07	2.42338E-07	1.14475E-07					
1	1355	5.40749E-08									
1	1445	0.002									
1	1442	0.5									
1	1	1443	1.0	E-7						FLOAT	PT
1	1	1	2	1101	0.0	0.0015				DRIVE	1
	.10000E 01	.99987E 00	.99950E 00	.99889E 00	.99802E 00	.99692E 00					
	.99557E 00	.99397E 00	.99214E 00	.99007E 00	.98776E 00	.98522E 00					
	.98244E 00	.97943E 00	.97620E 00	.97275E 00	.96907E 00	.96518E 00					
	.96108E 00	.95677E 00	.95225E 00	.94753E 00	.94262E 00	.93752E 00					
	.93224E 00	.92677E 00	.92113E 00	.91532E 00	.90935E 00	.90322E 00					
	.89694E 00	.89052E 00	.88395E 00	.87726E 00	.87043E 00	.86349E 00					
	.85644E 00	.84928E 00	.84203E 00	.83468E 00	.82725E 00	.81974E 00					
	.81217E 00	.80453E 00	.79684E 00	.78910E 00	.78133E 00	.77352E 00					
	.76569E 00	.75785E 00	.75000E 00	.74214E 00	.73430E 00	.72647E 00					

```

.71866E 00 .71089E 00 .70315E 00 .69546E 00 .68782E 00 .68025E 00
.67274E 00 .66531E 00 .65796E 00 .65071E 00 .64355E 00 .63650E 00
.62956E 00 .62274E 00 .61604E 00 .60947E 00 .60305E 00 .59677E 00
.59064E 00 .58467E 00 .57886E 00 .57322E 00 .56775E 00 .56247E 00
.55737E 00 .55246E 00 .54774E 00 .54323E 00 .53891E 00 .53481E 00
.53092E 00 .53092E 00 .52724E 00 .52379E 00 .52056E 00 .51478E 00
.51223E 00 .50992E 00 .50785E 00 .50602E 00 .50442E 00 .51478E 00
.50197E 00 .50110E 00 .50049E 00 .50012E 00 .50000E 00
1 3 1 2 1101 0.0 0.0015 DRIVE 2
.10000E 01 .99987E 00 .99950E 00 .99889E 00 .99802E 00 .99692E 00
.99557E 00 .99397E 00 .99214E 00 .99007E 00 .98776E 00 .98522E 00
.98244E 00 .97943E 00 .97620E 00 .97275E 00 .96907E 00 .96518E 00
.96108E 00 .95677E 00 .95225E 00 .94753E 00 .94262E 00 .93752E 00
.93224E 00 .92677E 00 .92113E 00 .91532E 00 .90935E 00 .90322E 00
.89694E 00 .89052E 00 .88395E 00 .87726E 00 .87043E 00 .86349E 00
.85644E 00 .84928E 00 .84203E 00 .83468E 00 .82725E 00 .81974E 00
.81217E 00 .80453E 00 .79684E 00 .78910E 00 .78133E 00 .77352E 00
.76569E 00 .75785E 00 .75000E 00 .74214E 00 .73430E 00 .72647E 00
.71866E 00 .71089E 00 .70315E 00 .69546E 00 .68782E 00 .68025E 00
.67274E 00 .66531E 00 .65796E 00 .65071E 00 .64355E 00 .63650E 00
.62956E 00 .62274E 00 .61604E 00 .60947E 00 .60305E 00 .59677E 00
.59064E 00 .58467E 00 .57886E 00 .57322E 00 .56775E 00 .56247E 00
.55737E 00 .55246E 00 .54774E 00 .54323E 00 .53891E 00 .53481E 00
.53092E 00 .52724E 00 .52379E 00 .52056E 00 .51755E 00 .51478E 00
.51223E 00 .50992E 00 .50785E 00 .50602E 00 .50442E 00 .50307E 00
.50197E 00 .50110E 00 .50049E 00 .50012E 00 .50000E 00
0 0 0 0 5 2 1 0 0.0 0.2 DRIVE 3
0 0 0 0 4 2 1100 .152 DRIVE 4
0 0 0 0 4 2 1 3 10.0 DRIVE 5
PROBEND END

```

The problem is identified as an initially subcritical system (KUSOR = 2, address 7 in fixed-point data) so that an initial external-source distribution (EXOR, EXSORB, addresses 1161-1310 and 1311-1329 in floating-point data) and emission spectrum (CHIEX, addresses 1330-1359 in floating-point data) must be given. The maximum number of inner iterations (MAXIN = 300, address 8 in fixed-point data) has been raised from the default value of 100. Amplitude edits (KUDUMP = 3, address 19 in fixed-point data) will be taken at intervals of at most 0.03 sec (DUMPT = 0.03, address 10 in floating-point data); shape edits will be taken at each shape step. See Section VII.B. for details of these edits.

Note that the composition assignment to spatial region (MIR, address 112-130 in fixed-point data) shows composition 1 assigned to both regions 1 and 3. A composition may appear in any number of regions. However, the code treats the composition in each region as a separate entity whose properties, such as temperature and volume fractions of component mixtures, can vary independent of the properties of the same composition in another region. Also note that the problem termination time (FINT, address 7 in floating-point data) is entered twice. The last value encountered in the input deck applies; the order of appearance of fixed- and floating-point data entries is otherwise unimportant. The last card of each of these blocks must, however, have a nonzero entry in columns 3-4.

The driving-function data include two tabular functions (DRIVE 1 and DRIVE 2), one fixed-shape-interval specification (DRIVE 3) with an interval of 0.2 sec, a shape recalculation forced at 0.152 sec (DRIVE 4), and a trigger function

(DRIVE 5) which turns off function DRIVE 3 at a problem time of 10 sec. Functions DRIVE 1 and DRIVE 2 will be turned off, and therefore force a shape recalculation, at 0.150 sec, since they each have 100 intervals of length 0.0015 sec between tabulated values.

This problem required high-accuracy flux values, so that many shape functions were calculated. The main controlling factor was the fixed-shape interval driving function DRIVE 3, which forced 50 shape-function recalculations. A total of 68 flux shapes were calculated; however, since the flux shape was changing very little, the number of inner iterations per step was small. The execution time of the dynamic solution on the CDC-3600 machine was 29 min. The job was not rerun on the IBM 360/75, but based on other cases the corresponding execution time is estimated to be 10 min on that machine. The problem was rerun on the CDC-3600 with the time interval value of function DRIVE 3 increased from 0.2 to 0.4 sec. At all common time points, all quantities with exception on instantaneous inverse period agreed to at least five digits. The inverse period varied from  $10^{-4}$  to  $10^{-2}$   $\text{sec}^{-1}$  in the time range of the comparison, where it represented differences of terms of the order of  $10^{-4}$ .

## VII. OUTPUT

A. Printed Output

Detailed description of the available printout would be a prodigious and somewhat wasteful task. All output numbers are tagged with Hollerith identifiers which are self-explanatory in most cases. The following comments are addressed to those items which are not obvious or are not described elsewhere in this report.

The first item, "Steady-state Reactivity Residue," appears in the  $t = 0$  edit of the dynamic solution. This quantity is given by Eq. 39 and is a result of approximations discussed in Section III.C.2. The output entry titled RHO is the sum of  $\rho + (k_0 - 1) / k_0$ , as given in Eq. 36.

The edit lines titled "ROSTEP n" are given at the end of each reactivity time step  $\Delta t_i^n$ , and represent the final results after the outer, or j-level, iteration has converged. In each of these edit blocks there are two or three items which require explanation. The item titled "ENERGY (MWS)" represents the total energy generated up to the given time in excess of that which would have been generated under initial steady-state conditions. The value always will be equal to zero unless the fuel-temperature routine is active (see Section VIII). Since this value is computed from the first j-iterate values of  $N^{(j)}(t)$ , it contains an error roughly proportional to the error in the integral of  $N^{(j)}(t)$  between the first and the final j iterations. This error, expressed as

$$PERCENT\ ERROR = 100x \frac{\int_{t_i^B}^{t_{i+1}^B} [N(t) - N^{(1)}(t)] dt}{\int_{t_i^B}^{t_{i+1}^B} [N(t)] dt} \quad (68)$$

is printed with the edit at the beginning of the following shape interval.

The entry "MAXORD k" in the  $t_i^n$  edit indicates the finest subdivision of the  $\Delta t_i^n$  interval which occurred in the point-kinetics routine. This minimum interval is given by

$$\left(\Delta t^k\right)_{\min} = \Delta t_i^n \times 2^{-(k-1)} \quad (69)$$

where k is the value printed.

A shape-function edit line is printed immediately following the title "BEGIN SHAPE STEP." This line identifies the shape test number (see Table V) that caused the shape recalculation, and the time of the shape calculation. In

addition, for each j iteration, values are given for the number of flux iterations, the estimate of the dominance ratio of the equivalent homogeneous equation, and the  $\gamma$  factor of the iteration. The maximum number of j iterations currently is limited to five. This was done to avoid looping in such cases as a superprompt critical burst followed by a low-power time range. Errors in spatial precursor concentrations which were accumulated in the burst can affect the following low-power solution such that  $\gamma$  will not converge to 1.0. The only remedy at present is to use narrower  $\Delta t^B$  spacing in the high-power time range. A more satisfactory remedy would be a j-iteration update of the spatial precursor concentrations; however, this would increase running time appreciably.

## B. Permanent Files

### 1. Amplitude Data

An input option (KUDUMPT, address 19 in fixed-point data) is set to obtain an amplitude-equation edit on specified time intervals. According to the time interval given in the input data (DUMPT, address 10 in floating-point data), the amplitude edit is taken at each  $t_i^k$  point which is the nearest larger value to one end point of the constant-spacing time mesh defined by interval DUMPT. The edit also is taken at every  $t_i^n$  point. The structure and content of the amplitude edit record are given in Section X.A.2.

### 2. Shape-function Data

This edit is taken at each  $t_j^B$  time point, including the initial value at  $t = 0$ . This edit is taken only if the option KUDUMPT is greater than 1. Structure and content of the shape edit record are given in Section X.A.3.

## VIII. FUEL-TEMPERATURE CALCULATION

The purpose of the fuel-temperature routine was to test the code performance in the presence of feedback. Temperature feedback was chosen because it produces a prompt response, which is the most difficult to treat.

The average power density in region R at time t is given by

$$P_R(t) = \frac{g_R}{V_R} \left[ \int_R \sum_g \sigma_g^f \psi(\vec{r}, t) d\vec{r} \right] N(t) \quad (70)$$

where  $g_R$  is the reduction factor to account for transverse power shape and  $V_R$  is the region volume. With the assumption that the heat-removal rate remains constant at the rate at  $t = 0$ , the excess energy density in units of  $W - sec/cm^3$  in interval  $\Delta t_i^n$  is

$$E_R(\Delta t_i^n) = \frac{g_R}{V_R} \left[ \int_R \sum_g \sigma_g^f \psi_g(\vec{r}, t_{i-1}^n) d\vec{r} \int_{t_{i-1}^n}^{t_i^n} N(t) dt - (t_i^n - t_{i-1}^n) \int_R \sum_g \sigma_g^f \psi_g(\vec{r}, 0) d\vec{r} \right] \frac{1}{2.91 \times 10^{10}} \quad (71)$$

where the power shape at the beginning of interval  $\Delta t_i^n$  approximates the true shape in the interval.

The fuel temperature rise resulting from this excess energy is given by

$$\Delta T_R = \frac{H_F}{F_F} E_R(\Delta t_i^n) \quad (72)$$

where  $H_F$  is the heat capacity of the fuel in  $(cm^3 - ^\circ K / W - sec)$  and  $F_F$  is the volume fraction of fuel in the region. Thus all the energy is assumed to appear in the fuel, and none of the excess energy is dissipated from the fuel. All mixtures in the region which are identified as fuels by the Hollerith designations "FISS" or "FERT" (see Section VI.A.4) will be increased in temperature by increment  $\Delta T_R$ .

## IX. QX1 CROSS-SECTION FILE

A. Card Input

If the variable NTAPE (see Section VI.A.2) is equal to 2, these data are placed between the Isotope-to-Mixture specifications (Section VI.A.4) and the Mixture-to-Composition specifications (Section VI.A.6). The control cards (types a-l below) must be input of cards; the cross-section data may follow directly, or be input from logical unit 1. The routines prepare a QX1-format library file on logical unit 2; this unit may be saved as a permanent library. A single weighting spectrum may be used to collapse to fewer energy groups if desired. Card input may be in either XLIBIT (Ref. 22) of MC<sup>2</sup> (Ref. 25) formats, or a mixture of the two.

<u>Card</u>	<u>Format</u>	<u>FORTRAN Name (dimension)</u>	<u>Description</u>
a	I6	NTP	Set equal to 60 if the cross-section decks are to be input directly. Set equal to 1 if the cross-section card images are input from logical unit 1.
b	A5	ANO	Cross-section set name.
	IX		Blank.
	I6	MATLS	Total number of isotopes in input set.
	I6	NGPS	Number of groups in input set.
	I6	NDN	Number of downscatter groups in input set. (Scattering cross sections to groups with index greater than J + NDN will be added to the cross section for scatter from J to J + NDN.)
	I6	NCOL	Number of groups in collapsed set. If zero, no collapsing will be done.
	I6	NTROP	1: collapse $\sigma_{tr}$ linearly with $\phi$ . 2: collapse $1/\sigma_{tr}$ linearly with $\phi$ . 3: use Travelli definition <sup>24</sup> of collapsed microscopic $\sigma_{tr}$
	I6	NFGER	If MC <sup>2</sup> input is used, enter the total Number of groups in the card input.

(This may be used to delete the unnecessary thermal group; i.e.,  $NFGR = NGPS + 1$ ).

	I6	IANO	Set equal to 1 if the cross-section set contains anisotropic scatter. An isotropic set will be produced.
	I6	NDIF	If $NCOL \neq 0$ , $NTROP = 3$ , $NDIF \neq 0$ , enter $D = 1 / (3\sigma_{tr})$ on Card f.
c	2413	NRLK(500)	Format cue for the Lth isotope. Enter 0 for XLIBIT format, 1 for $MC^2$ format. (Enter MATLS numbers, 24 per card.)

The following three card types are required if  $NCOL \neq 0$ .

d	2413	ID(30)	The fine-group index of the lowest-energy fine group within broad group I. (Enter $NCOL$ numbers.)
e	6E12.5	PHI(30)	Fine-group spectrum for group collapse. (Enter $NGPS$ numbers.)
f	This card type is required only if $NTROP = 3$		
	6E12.5	HOMTR(30)	The homogenized fine-group transport cross section for the "reference" composition. (See NDIF above.)

Card formats may be either  $MC^2$ , XLIBIT, or a combination of the two. If the first isotope is in  $MC^2$  format, two extra pieces of input must be entered.

<u>Card</u>	<u>Format</u>	<u>FORTRAN Name (dimension)</u>	<u>Description</u>
g	6E12.5	CHI(30)	Prompt-neutron emission fraction for group j. Enter $NGPS$ numbers.
h	6E12.5	VELOC(30)	Mean neutron velocity for group j. Enter $NGPS$ numbers.

The isotope name will be taken from the first five columns of the first card in the  $MC^2$  format. The format of this card becomes (A5, 1X, I6, 12X, 6A8,

A2). The A-field may be used for identification; this string will be listed by QXLIB2.

FORTRAN			
<u>Card</u>	<u>Format</u>	<u>Name (dimension)</u>	<u>Description</u>
i	A6	SIGND	The six Hollerith characters SIGEND in card columns 1-6.

These cards are followed by MATLS cross-section decks. If NTP = 60, these decks are placed in the input stream, between card type h and card type i. If NTP = 1, the card images must be available on LUN01, and card type i immediately follows card type h. Temperature-dependent cross sections must be entered sequentially in order of increasing temperature; if the isotope is fissionable, QX1 assumes that the capture and fission cross sections are temperature-dependent. If less than four isotopes with the same first five characters in their isotope labels are grouped together, the capture and fission cross sections of the last one encountered are entered into the locations for higher temperature values. For example, if only one such isotope is present, its capture and fission cross sections will be entered in all three higher temperature values.

## B. Structure and Content of Cross-section File

1. File 1 Structure. One Record Type 1, followed by a block for each isotope consisting of one Record Type 2, one Record Type 3, and three Record Type 4 (conditional).

### Variable Name      Description

- a. Record Type 1: GRAT

GRAT                      Five-character Hollerith set name

- b. Record Type 2: AMATNI,LFIS

AMATNI                    Five-character Hollerith isotope name.

LFIS                        Fission flag. Zero indicates nonfissionable; one indicates fissionable.

- c. Record Type 3: (CRUD(I)=1,331),(TRANI(J),J=1,NOG),  
(CAPI(J,I),J=1,NOG),(FISI(J,1),J=1,NOG),  
(GNUI(J),J=1,NOG).

CRUD(I) Scattering matrix position I. If  $\sigma_{gg'}$ , is the scattering cross section from group  $g'$  to group  $g$ , then when  $g \leq 15$ , it is stored in location  $I = g' - g + 2 + \sum_{k=1}^{g-1} k$  when  $g > 15$ , it is stored in  $I = g' \cdot g + 107 + 15(g - 15)$

TRANI(J) Transport cross section ( $\sigma_g^{tr}$ ) for group  $J$

CAPI(J,1) Capture cross section ( $\sigma_g^c$ ) at temperature  $T_1$

FISI(J,1) Fission cross section ( $\sigma_g^f$ ) at temperature  $T_1$

GNUI(J) Total neutron yield per fission ( $\nu_g$ )

- d. Record Type 4: (only if LFIS=1) (CAPI(J),K),J=1,NOG), (FISI(J,K),J=1,NOG).

CAPI(J,K) Capture cross section ( $\sigma_g^c$ ) at temperature  $T_K$

FISI(J,K) Fission cross section ( $\sigma_g^f$ ) at temperature  $T_K$

2. File 2 Structure. Three records.

Variable Name    Description

- a. Record Type 1: NOG,NOD,ITOT

NOG                    Number of energy groups

NOD                    Maximum number of downscatter groups

ITOT                    Number of isotopes in set

- b. Record Type 2: (TOPE(I),I=1,ITOT),(INUM(I),I=1,ITOT).

TOPE(I)                Hollerith (five-character) name of isotope I.

INUM(I)                The record number of the first record of isotope I data in File 1.

- c. Record Type 3: (VEL(J),J=1,NOG),(CHIP(J),J=1,NOG).

VEL(J)                    Neutron velocity in energy group J

CHIP(J)                      Prompt-neutron emission fraction to energy group J

C.        Limitations on Cross-section File

The following is a list of specific limitations on the structure and content of the basic cross-section library which may be used to prepare a QX1 library. The limitations are given in terms of the CDC-3600 XLIBIT file, but they apply generally to any cross-section input.

Maximum of 320 isotopes

Maximum of 30 energy groups

Maximum of 15 downscatters

The prompt chi's can be group-dependent only, and must be identical for all isotopes. (The last chi block takes precedence.)

Upscattering is not allowed

Elastic, inelastic and n,2n downscattering is allowed for and  $\ell$  order of 0 only.

The self-scattering term is neglected.

If a Standard XLIBIT File Is Used

(a) The isotope name is referenced as the first A5 of the A6 name. Any blanks present on the left of the isotope names in the original file will be squeezed out until the isotope name is left-adjusted in the field. Therefore, all references to the isotopes in the Mixture Data (Section VI.A.6) must be left-adjusted in order to match the cross-section file names.

(b) Any fuel isotopes have their  $\sigma^c$  and  $\sigma^f$  set at all four temperatures.

If an XLIBIT Tape (QX1 Version) Is Used

(a) The A6 isotope name becomes A5, the sixth character being filled (with 1,2,3,or 4) for fuel isotopes only.

(b) The isotopes may appear in any order, except that once a fuel is present it must be followed immediately by the three related fuels (for T2, T3 and T4 –in that order).

(c) If any of the three related fuels are missing  $\sigma^c$  and  $\sigma^f$  of the last one encountered are entered for the missing values.

## X. SCRATCH FILES

A. Logical Unit 03

This file is used to store the amplitude function during the first iteration on the shape-function interval. If a problem dump is requested, dump information is moved to LUN03 from LUN08 and LUN09 at the end of the problem.

1. Run-Time Structure. One Record Type 1, one Record Type 2, (N-1) Record Type 3, where N is the number of reactivity-recalculation intervals in the shape-function interval.

<u>Variable Name</u>	<u>Description</u>
----------------------	--------------------

- a. Record Type 1: TMIN,(PREC(K),K=1,NOF),DT1,AMPI,  
(AMPVA(I),I=1,3),ALPHA.

TMIN	Time at start of shape interval $t_0^B$
PREC(K)	Integrated precursor density in family K at TMIN
NOF	Number of delayed-neutron precursor families
DT1	Time interval preceding time TMIN
AMPI	Amplitude function of TMIN
AMPVA(I)	Logarithm of amplitude function at last three time points
ALPHA	Instantaneous inverse period of amplitude function at TMIN

- b. Record Type 2: TMAX,((BETVA(I,K),I=1,3),K=1,NOF),  
(ROVA(I),I=1,3),(PROLVA(I),I=1,3),  
(EXVA(I),I=1,3),ETOT,(VAT(I,1,1),  
I=1,640).

TMAX	Time at end of first interval $(t_1^n)$ . $\beta_s / \Lambda$ at time point I, where I is the index of time TMIN – DT <sub>i</sub> , TMIN, and TMAX.
ROVA(I)	$\rho / \Lambda$ at time point I
PROLVA(I)	$\Lambda$ at time point I

EXVA(I)	$Q' / F\Lambda$ at time point I
ETOT	Total excess-energy generation from time zero to time TMAX.
VAT (I,1,1)	Regional volume fraction and temperature array for each mixture at time TMAX.

- c. Record Type 3: TMAX,(BETVA(3,K),K=1,NOF),ROVA(3),  
PROLVA(3),ETOT,(VAT(I,1,1),I=1,640).

TMAX	Time at end of current reactivity recalculation interval
BETVA(3,K)	$\beta_s / \Lambda$ at TMAX
ROVA(3)	$\rho / \Lambda$ at TMAX
PROLVA(3)	$\Lambda$ at TMAX
EXVA(3)	$Q' / F\Lambda$ at TMAX
ETOT	Total excess energy up to time TMAX
VAT(I,1,1)	Volume fractions and temperatures at TMAX

2. Dump Structure; File 1. (Present if KUDUMPT = 1 or 3.) One Record Type 1, followed by a number of Record Type 2 equal to total number of reactivity recalculation steps plus intermediate points when input interval DUMPT is less than the reactivity step length.

Variable Name      Description

- a. Record Type 1: (BCD(I),I=1,10)

BCD                      Problem title card image

- b. Record Type 2: TIME,AMPI,ALPHA,RHO,PROL,SEXT,  
(BETA(K),PREC(K),K=1,NOF).

TIME                     Dump time

AMPI                    Amplitude function ( $N$ )

ALPHA                  Instantaneous inverse period of amplitude function

RHO	Reactivity ( $\rho$ )
PROL	Generation time ( $\Lambda$ )
SEXT	Integrated external source ( $Q / F\Lambda$ )
BETA(K)	Effective delayed-neutron fraction of family K
PREC(K)	Integrated precursor density in family K
NOF	Number of delayed-neutron precursor families

3. Dump Structure; File 2. (Present if KUDUMPT = 2 or 3.) One Record Type 1, followed by a number of Record Type 2 equal to the number of shape-function recalculation steps.

- a. Record Type 1: (BCD(I),I=1,10),(MAB(M),DELR(M),M=1,NOR)

BCD	Problem title-card image
MAB(M)	Mesh-point number at outer boundary of region M
DELR(M)	Mesh spacing in region M
NOR	Number of regions in problem

- b. Record Type 2: TCUR,AMPI,((FIS(J,M),J=1,NOG),M=1,NOR),((PHI(J,N),J=1,NOG),N=1,NOP),((C(N,K),N=1,NOP),K=1,NOF0,((CB(M,K),M=1,NOR1),K=1,NOF).

TCUR	Current Time
AMPI	Amplitude function
FIS(J,M)	Fission cross section in group J, region M
NOG	Number of groups
PHI(J,N)	Flux-shape function in group J, mesh point N
C(N,K)	Precursor density at mesh point N, family K
NOF	Number of delayed-neutron precursor families

CB(M,K) Precursor density at inner boundary of region (M+1), family K

NOR1 (NOR – 1), number of regions minus 1

B. Logical Unit 04

This unit contains the driving-function specifications.

1. Structure In each of NUMI blocks (where NUMI is the number of driving functions), one Record Type 1, followed (conditionally) by either one Record Type 2 or one Record Type 3.

Variable Name    Description

- a. Record Type 1:    MODMAT,MODREG,KUEMAT,KUEREG  
MOD,KOP,KTRIG,NMI

MODMAT            Mixture number to be modified

MODREG            Region number of MODMAT

KUEMAT            Mixture number of trigger

KUEREG            Region number of KUEMAT

MOD                Function type

KOP                Trigger logic

KTRIG             Trigger test type

NMI                Modifier data type

- b. Record Type 2:    (Present if NMI=0 and MOD ≠ 4 or 5.)  
ANUMN,(MIVA(I),I=1,3).

ANUMN            Hollerith-function identifier

MIVA(I)            For I = 1,2,3, the coefficient A,B,C of the analytic function.

- c. Record Type 3:    (Present if NMI ≠ 0 and MOD ≠ 4 or 5.)  
DTMI,(SCRAP(I),I=1,NMI).

DTMI                    Time interval between data points

SCRAP(I)                Value of the driving function at time point I

C.        Logical Unit 08

This file is used to store the amplitude-function data during problem running when KUDUMPT = 1 or 3. Its structure is identical to Record Type 2 of file 1 on LUN03 (see Section X.A.2).

D.        Logical Unit 09

When NTAPE = 2 (see Section VI.A.2), the cross-section input cards are transferred to LUN09 before processing.

During running of the problem, this file contains the shape-function dump information if KUDUMPT = 2 or 3. Its structure is identical to Record Type 2 of file 2 on LUN03 (see Section X.A.3).

E.        Logical Unit 10

Scratch storage of the mixture cross sections and the adjoint flux.

1. Structure. One Record Type 1 and one Record Type 2.

a. Record Type 1: (SIGS(I,1),I=1,9616).

SIGS(I,1)                Location I in the mixture cross-section data. The index I range covers variables SIGS,SIGC,SIGT,SIGF,SIGN,DOPCP and YIELD.

b. Record Type 2: (APHI(I,1),I=1,4500).

APHI(I,1)                Location I of the adjoint flux

F.        Logical Unit 50

Used to store the steady-state real parameters during the adjoint solution, and to store the previous shape function during the dynamic solution.

1. File Structure; Steady State One Record Type 1 and one Record Type 2.

Variable Name        Description

a. Record Type 1: ((PHI(J,N),J=1,NOG),N=1,NOP),(FISOR(N),

N=1,NOP),(FISORB(M),M=1,NOR1),((C(N,K),  
N=1,NOP),K=1,NOF),((CB(M,K),M=1,NOR1),  
K=1,NOF),(OMEGI(J),J=1,NOG),(OMEGO(J),  
J=1,NOG).

PHI(J,N)	Steady-state shape function, group J, mesh point N
NOG	Number of groups
NOP	Number of points
FISOR(N)	Real fission source at point N
FISORB(M)	Real fission source at inner boundary of region (M+1)
NOR1	Number of regions minus 1
C(N,K)	Precursor density at point N, family K
NOF	Number of delayed-neutron precursor families
CB(M,K)	Precursor density at inner boundary of region (M+1)
OMEGI(J)	Inner-boundary extrapolation length, group J
OMEGO(J)	Outer-boundary extrapolation length, group J
b. <u>Record Type 2:</u>	((SCAT(L,M),L=1,331),M=1,NOR),((DIF(J,M), J=1,NOG),M=1,NOR),((ABSO(J,M),J=1,NOG), M=1,NOR),((PNUS(J,M),J=1,NOG),M=1,NOR), ((DNUS(J,K,M),J=1,NOG),K=1,NOF),M=1, NOR).
SCAT(L,M)	Scattering matrix, region M
DIF(J,M)	Diffusion coefficient, group J, region M
ABSO(J,M)	Capture plus fission
TOTR(J,M)	Total removal
PNUS(J,M)	Prompt neutrons/fission x fission cross section
DNUS(J,K,M)	Delayed neutrons/fission x fission cross section, group J, family K, region M

2. File Structure; Dynamic Module One recordVariable Name    Descriptiona. Record Type 1: TPL,((PLAST(J,N),J=1,NOG),N=1,NOP).

TPL                    Time of calculation of shape function

PLAST(J,N)           Previous shape function, group J, mesh point N

## XI. SUBROUTINE DESCRIPTIONS

Table VIII is a general guide to the function of each of the QX1 routines. Descriptions of each of the major operations are given on comment cards in the code listing.

TABLE VIII. QX1 Subroutines

Subroutine	Module	Called From	Purpose	Formal Parameters
ADIA	Dynamic	GOGO	Initialize fuel temperature calculations	PIN: Incremental energy in W-sec ITS: Iteration flag DERV: Maximum energy derivative, $\frac{\Delta T}{N\Delta t}$
AMPEDT	Dynamic	STEPIT GOGO	Print amplitude data	RFZ: Amplitude function integral NOF: Number of precursor families NOSTEP: $\Delta t^n$ step number TCUR: Time AMPO: Amplitude function ALPHA: Inverse period ETOT: Total excess energy MAXORD: Point-kinetics interval RO: Reactivity PROL: Generation time EXVA: External source BETA: Delayed-neutron fractions PREC: Precursor densities KUMP: Material print cue PHINT: Flux integral DT: Time step
ARBIT	Static	CRIT	Form second criticality search guess	PARM: Search parameters EFFK: Eigenvalues ERR: Current eigenvalue minus one Same as ADIA
BATIC (entry In ADIA)	Dynamic	GOGO	Calculate changes in fuel temperatures	
BOUND	Dynamic	DEL	Find boundary contributions to reactivity	KON: Boundary-condition flag B: Sign of surface normal PHI: Boundary fluxes APHI: Boundary adjoints DIF: Diffusion coefficients OMEG: Extrapolation length R: Boundary radius MAKE: Geometry type PIM: Geometry multiplier GRAL: Boundary contribution to p LINK: Control cue (see Section XII)
CALP	Dynamic	DYNAM GOGO	Calculate spatial precursor densities.	
COLAPS	Setup	QXTP2	Collapse cross sections.	NPUN: Dummy (unused) NTROP: Transport cross-section Collapse option
CRIT	Static	STATIC	Modify search parameter to find critical state.	None
DATIN	Setup	SETUP	Read data cards for compositions	None

DEFINE	Setup	SETUP	fixed- and floating-point data, and driving functions. Edit data. Complete input edit, calculate pre-defined quantities, call MACMIX(0) for initial cross sections.	None
DEL	Dynamic	DYNAM GOGO	Calculate reactivity and other inner products.	ISTORE: Store cue for regional integrals (see Section XII)
DRIVER	Root		Control overall calculation.	None
DYNAM	Dynamic	DRIVER	Drive dynamic solution.	None
EDIT	Setup	QXLIB2	Edit cross-section preparation.	L: Cross-section deck number KCUR: Isotope number AMAT: Isotope name TYPE: Isotope description label
EF	Dynamic	ROMBI	Find argument for Romberg integration routine.	X: Time ARG: Result AMPCO: Amplitude-function interpolation coefficients ITS: Iteration flag DT1: Previous time interval
ELASPE (entry in TIMER)	Root	SETUP STATIC DYNAM	Find computation time elapsed since last call.	Same as TIMER
GENSCH	Static	CRIT	Find general criticality-search trial parameter.	PARM: Search parameters EFFK: Eigenvalues ERR: Current-eigenvalue minus one
GOGO	Dynamic	DYNAM	Carry out first iteration of amplitude solution and next shape step.	None
INTERP	Dynamic	PULST MIF	Interpolate driving functions.	VALTR: Trigger time
LIBIN	Setup	SETUP	Read cross-section library, and form mixture cross sections.	None
LOGLIN	Static	CRIT	Find third criticality-search parameter.	PARM: Search parameters EFFK: Eigenvalues ERR: Current eigenvalues minus one
MACMIX	Root	DEFINE CRIT DYNAM GOGO	Form regionwise macroscopic cross sections.	IBUFF: Flag controlling adjoint flux read (see Section XII)
MIF	Dynamic	GOGO	Modify reactor parameters, or set time steps according to driving-function specifications.	ITS: Iteration flag NQU: Shape-function interval control (see Section XII)
NORMAL	Static	STATIC	Normalize real and adjoint fluxes. Initialize dynamic parameters.	None.
NUMC2	Setup	QXLIB2	Read cards in MC <sup>2</sup> format.	KCUR: Isotope number ISWEEP: Temperature-dependent isotope counter ANO: Cross-section set name LCT: File 2, LUN02 record count NUMF: Read count
PHIMOD	Dynamic	GOGO	Extrapolate flux-shape function.	PLAST: Previous shape function PHI: Current shape function TCUR: Current time TLOW: Time of PLAST IDS: Scratch file number (50)

POSE	Static	STATIC	Transpose cross-section matrices, invert group indices, and set up for adjoint solution.	NOG: Number of groups NOP: Number of mesh points None
PREGO	Dynamic	DYNAM	Set up next sequence of reactivity recalculation steps after a shape-function step.	XX: Shape-function computation time (sec)
PREPAR	Setup	SETUP	Initialize common blocks. Read title card, control card, delayed-neutron data, and mixture data.	None
PULSOR	Dynamic	RESHAP DEL	Calculate first-collision source at mesh point N, group J.	N: Mesh-point number J: Group number M: Region number ICALL: First-call flag STOR: Scratch area X1: Source
PULST	Dynamic	PULSOR	Calculate pulse intensity.	TIME: Time of neutron emission PULS: Pulse intensity NUM: Driving-function number for pulse shape STOR: Scratch area VALTR: Pulse initiation time ICALL: First-call flag
QXLIB2	Setup	SETUP	Read card-image cross sections, collapse if required, and prepare cross-section file on LUN02	None
QXTP2	Setup	NUMC2	Call COLAPS if required, and write File 1 of cross-section file on LUN02	KCUR: Isotope number LFIS: Fissionable-isotope flag ANO: Cross-section set name AMATNI: Isotope name ISWEEP: Temperature-dependent isotope counter LCT: File 2, LUN02 record count NUMF: Read count
REPR	Setup	DEFINE SHAPER CRIT POSE NORMAL RESHAP PREGO STEPIT AMPEDT	Print cross sections, composition data, shape function, or trouble dump, depending on value of NPR.	NPR: Print control
RESHAP ROMBI	Dynamic Dynamic	DYNAM GOGO	Calculate shape function. Integrate given function using Romberg algorithm.	None ALB: Lower integration limit UB: Upper integration limit D: Integral result KTFLUX: Dummy (unused) INTYPE: Dummy (unused) AMPCO: Amplitude-function ITS: Iteration flag DT1: Previous time step
SETUP SHAPER	Setup Static	DRIVER STATIC	Drive problem setup module Solve real and adjoint fluxes for initial steady-state conditions.	None None

SHAPUP (entry in PHIMOD)	Dynamic	RESHAP	Recover previous shape function shape extrapolation is used (KUDYS = 2).	Same as PHIMOD
STATIC	Static	DRIVER	Drive steady-state solution.	None
STEPIT	Dynamic	DYNAM	Solve point-kinetics equations for each shape calculation interval, and carry out second and subsequent amplitude solution iterations.	LOT: Flag for single step or iterative sweep. (see Section XII)
STNARG	Setup	QXLIB2	Read XLIBIT format card images	KCUR: Isotope number ISWEEP: Fissionable-isotope counter LFIS: Fissionable-isotope flag LCT: File 2, LUN02 record count NUMF: Read count
TESTER	Dynamic	GOGO	Test shape-calculation criteria, and estimate time at which shape function will be required.	CURVAL: Current values of parameter being tested OLDVAL: Parameter values at last shape step DTLIM: Estimated time interval remaining before criterion will be exceeded EPSEF: Prescribed limit on parameter change since last shape step NQU: Shape-recalculation flag NOR: Number of regions NUM: Shape test number
TIMER TRAP	Root Root	SETUP SHAPER RESHAP	Initialize computation timer. Trapezoidal integration	Z: Elapsed time (sec) since last call X: Function values FAC: Multiplicative factor R: Radius values DELR: Mesh spacing PIM: Geometry factor II: Lower-limit point LOOP: Upper-limit point M: Region number GRAL: Result
VFSUM	Static	CRIT	Total volume fractions of fuel and diluent mixtures during composition search.	NOM: Number of mixtures M: Region number INDEX: Internal/external mixture correspondence MFLAG: Search flags VAT: Volume-fraction/temperature array VPAR: Total fuel volume fraction VPAR2: Total diluent volume fraction
XLIBIN	Setup	SETUP	Read XLIBIT binary tape. (Relevant only in CDC-3600 version.)	None

---

## XII. PROGRAM STRUCTURE

The following is an introductory guide to the sequence of calculations in QX1. Major program control flags are given in Table IX, and calculation sequences are outlined by simplified flow charts (Figs. 2-7). The code listing itself is given as the reference documentation; comment cards have inserted at all key points to simplify reading of the listing.

TABLE IX. Major Program Control Flags

Variable Name	Description
IFLAG	Set equal to two in STATIC to indicate first pass through steady-state module. Set equal to zero in SHAPER to indicate real solution phase. Reset to one in POSE to initiate adjoint phase. This setting is used in the dynamic module to indicate the first pass of the dynamic solution. Reset to zero in GOGO for dynamic solution, and to two in PREGO for problem termination. If the initial steady-state problem is inhomogeneous and if a second steady-state iteration is required, it is set to zero in DYNAM as a branch indicator in DRIVER.
NIX	Set equal to two at a number of locations to indicate an unrecoverable error. Set to minus one in CRIT to indicate converged criticality search.
ITIN	Count on number of source iterations in SHAPER and RESHAP. Problem terminates when $ITIN \geq MAXIN$ .
ITOUT	Count on number of criticality search trials in SHAPER. Problem terminates from CRIT when $ITOUT > MAXOUT$ . Used in RESHAP to count number of iterations between amplitude and shape functions. If $ITOUT > 5$ , problem proceeds with unconverged values.
JAM(1)	Set in DYNAM to count number of iterations carried out to obtain consistent initial conditions in source problems. If greater than two, dynamic solution is initialed with unconverged values.
KEND	Input as zero or one to indicate problem end conditions. Set equal to two when these conditions are reached.
LINK	Call to CALP with $LINK = 0$ indicates that a shape-calculation step has been completed, and so CALP updates the spatial precursor integrands and returns. $LINK = 1$ indicates that a reactivity step is complete, and CALP updates the spatial precursor densities.
ISTORE	Call to DEL with $ISTORE = 0$ causes the regional integrals which are elements of various shape-calculation criteria to be stored for use as those calculated at the last shape step. A call with $ISTORE = 1$ causes the same integrals to be stored as those calculated at the end of a reactivity step.
IBUFF	Call to MACMIX with $IBUFF = 1$ causes adjoint to be read in MACMIX.
ITS	Iteration flag, set in GOGO to indicate that the reactivity recalculation step is being iterated because of nonconvergence of the extrapolated and calculated amplitudes at the end of the reactivity step.
NQU	Shape-recalculation flag, set in GOGO or MIF to force a shape calculation at the end of the current reactivity interval.
LOT	A call to STEPIT with $LOT = 1$ causes the amplitude function to be calculated over a single reactivity recalculation step. A call with $LOT = 0$ causes recalculation of all

steps from the time of the previous shape calculation up to the present time; that is, calculation of the second or subsequent iteration of the amplitude solution.

---

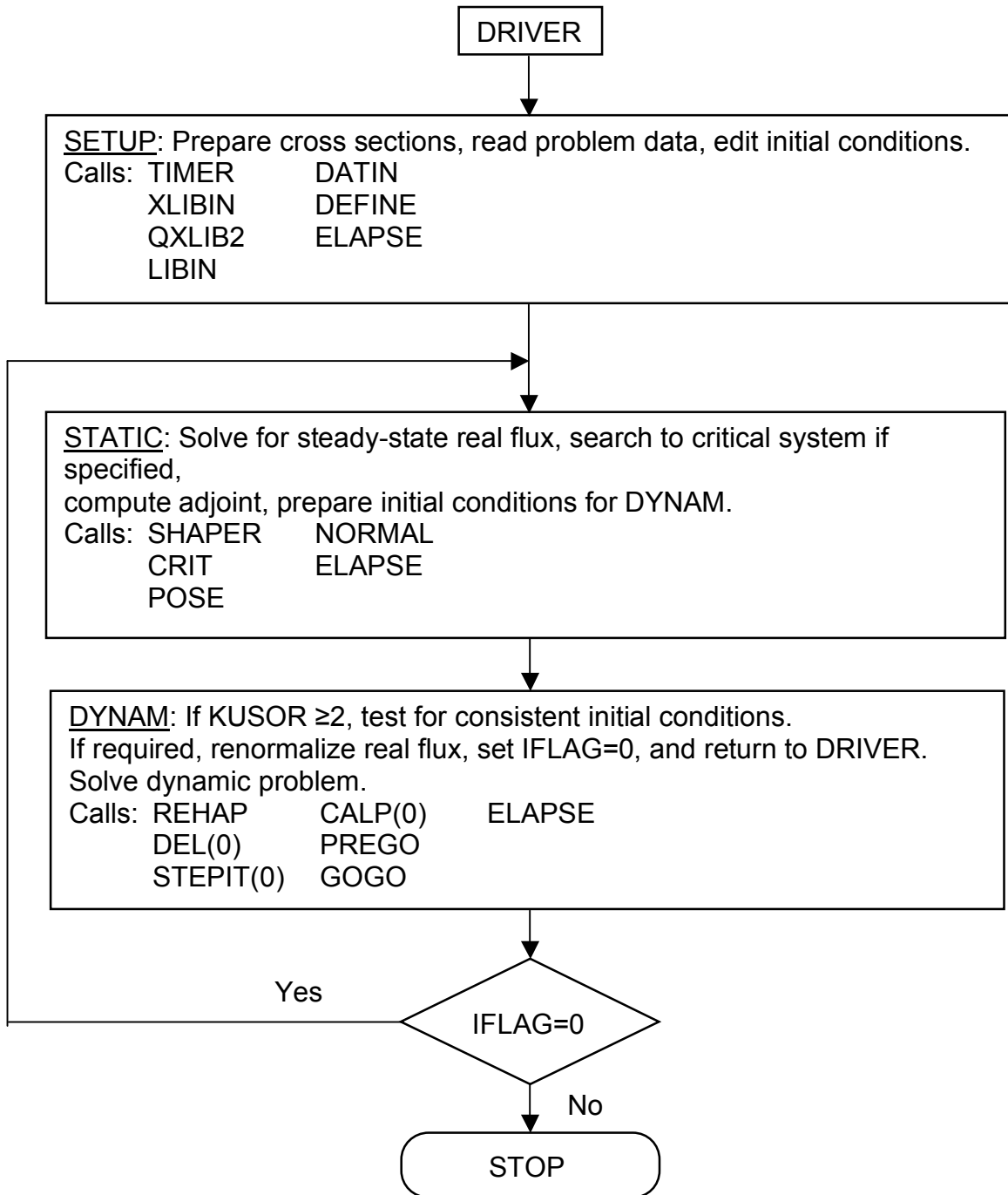


FIG 2. DRIVER Calling Sequence

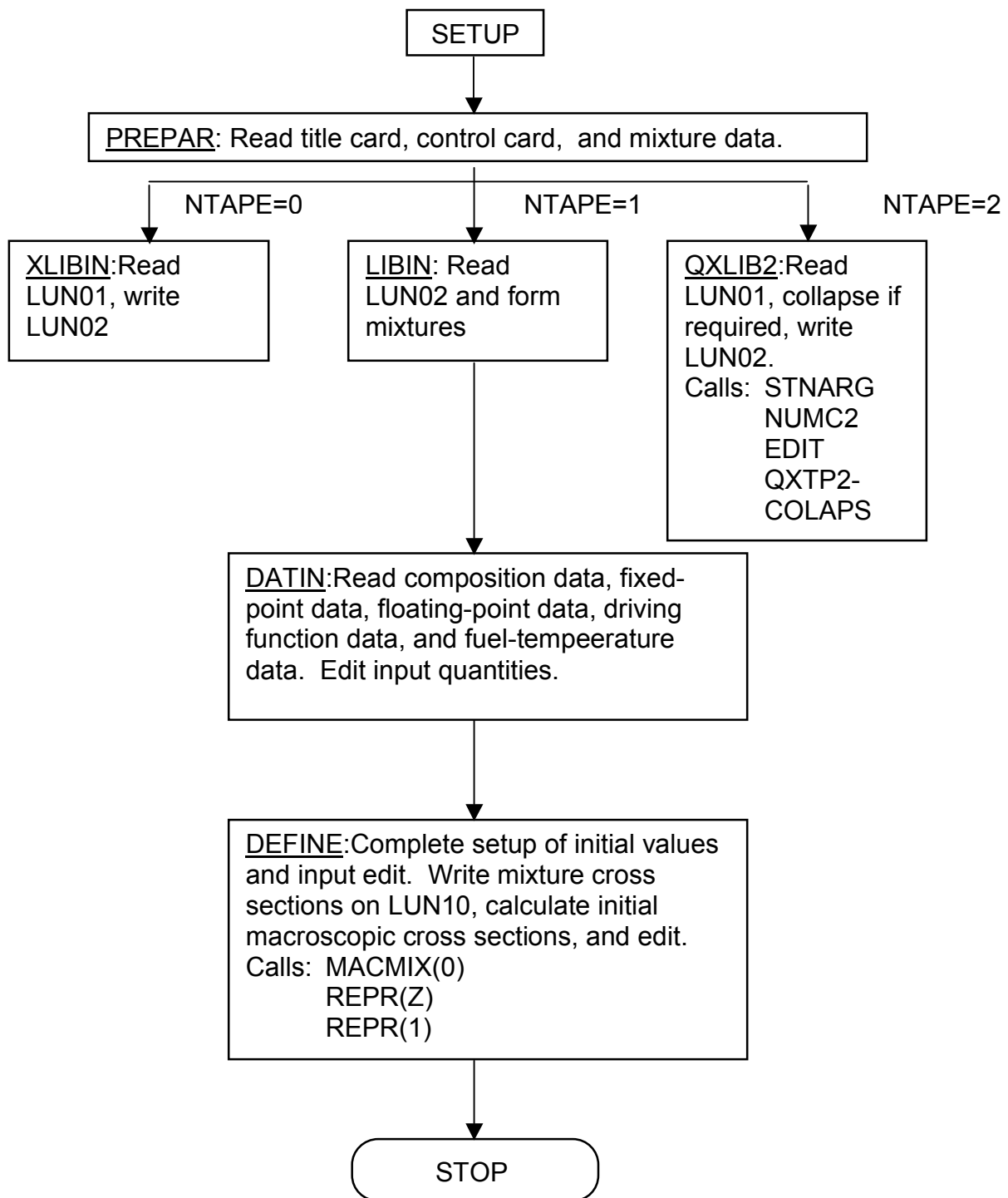


FIG 3. SETUP Calling Sequence

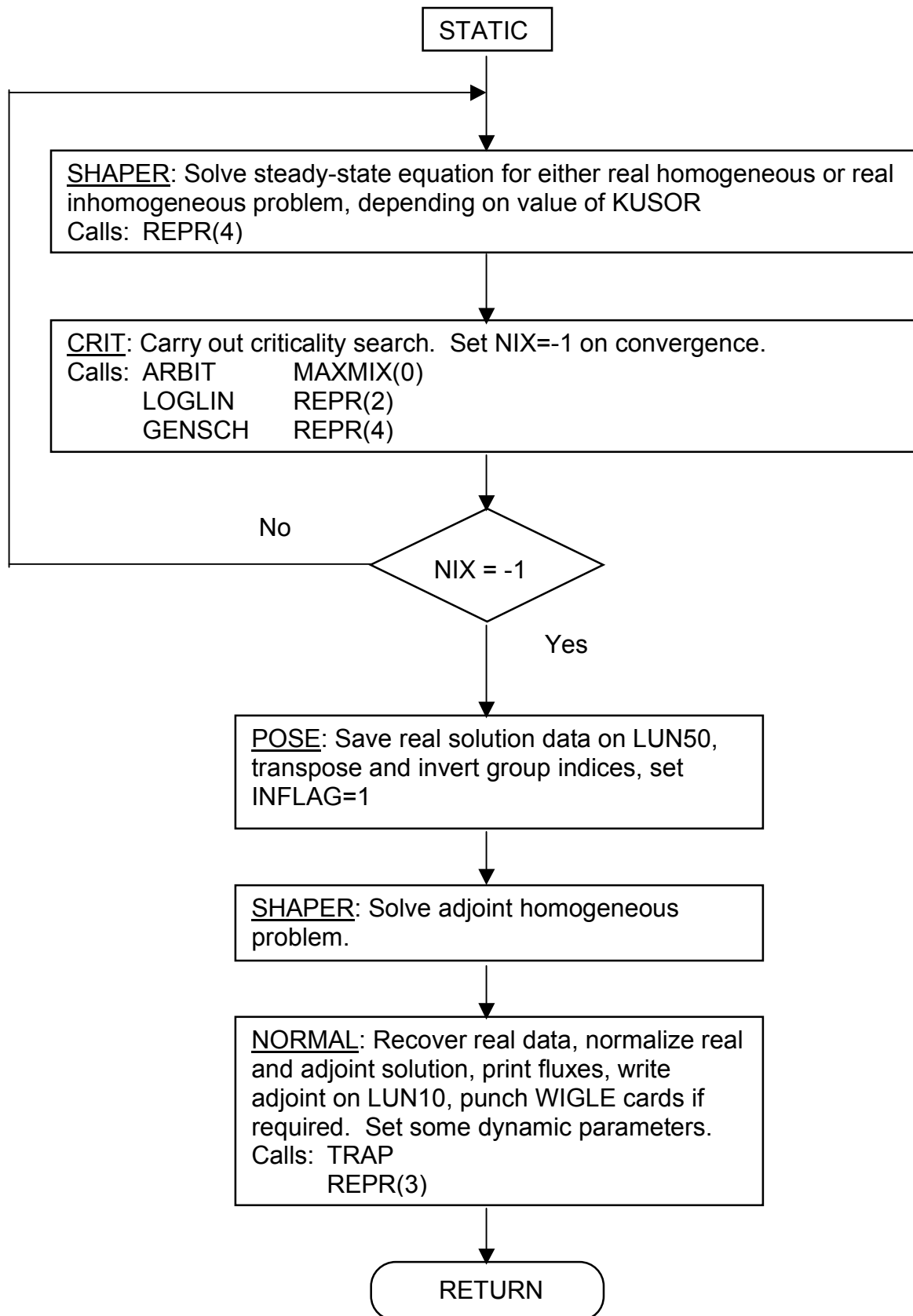


FIG 4. STATIC Calling Sequence

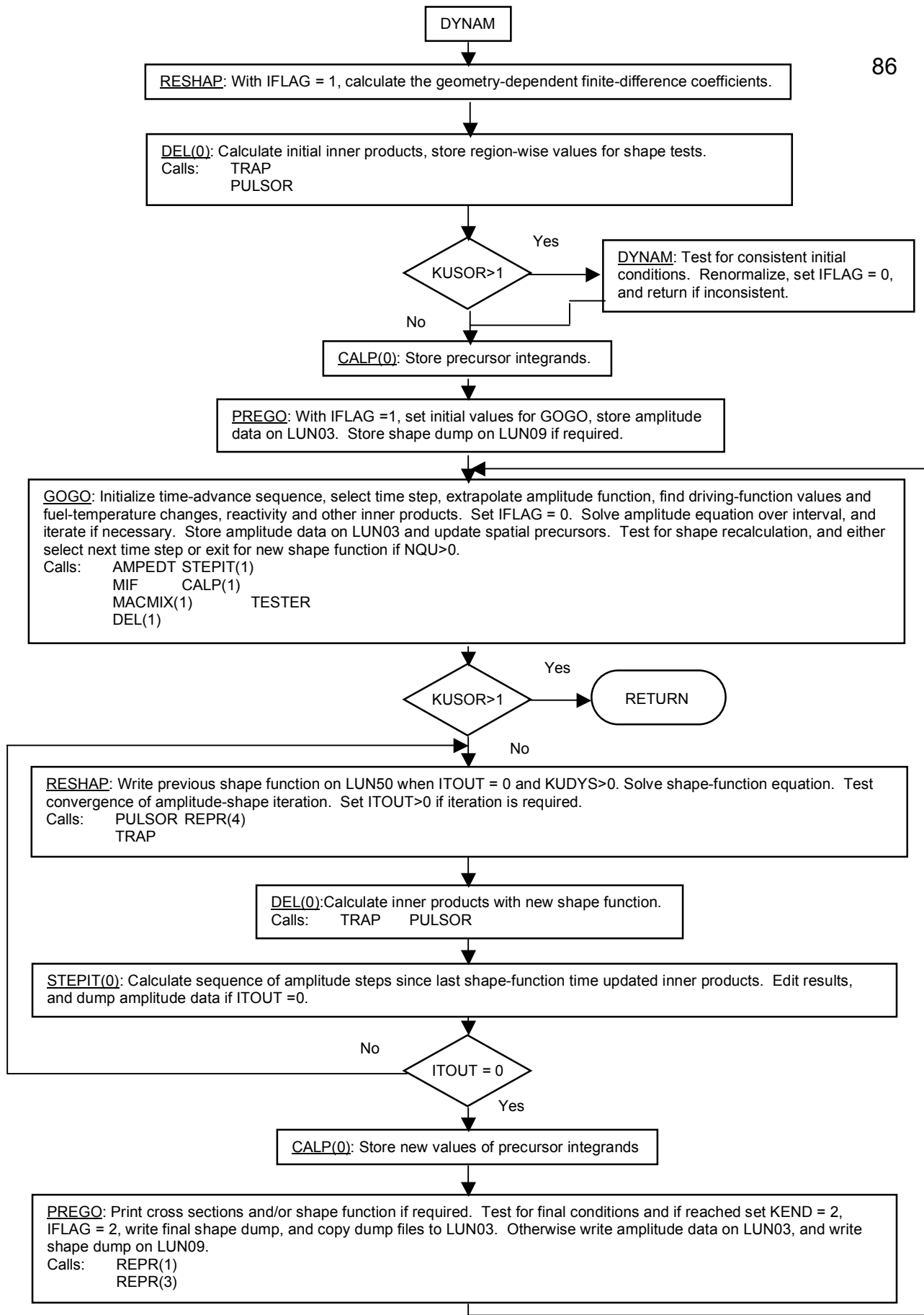


FIG 5. DYNAM Calling Sequence

## XIII. COMMON BLOCK DICTIONARY

<u>Variable Name (dimension)</u>	<u>Common Block No. (location relative to start of block)</u>	<u>Definition</u>
ABSO(30,20)	3(11721)	Group- and region-dependent (macroscopic) sigma-absorption (capture plus fission) array.
ALPHA	2(1160)	Current inverse period $\alpha(t)$
ALPHAB	3(13290)	ALPHA at the last shape-function step, $\alpha(t_{i-1}^B)$
AMPCO	3(13299)	Coefficients of the $1n$ N parabola, $a_1, a_2, a_3$ , used to extrapolate $N_{EX}$ as $1n N_{EX}(t) = a_1 + a_2(t - t_{i-1}^n) + a_3(t - t_{i-1}^n)^2$
AMPEX	3(13293)	Extrapolated amplitude ( $N_{EX}$ )
AMPI	3(13291)	Amplitude at the start of the reactivity time step
AMPIN	3(13294)	Integral of the amplitude, using the Unmodified (initial sweep) values of N, $\int_0^t N(t) dt$
AMPLIM	2(9)	Final amplitude value (if KEND=1). Calculation ends when $N(t_f) = \text{AMPLIM}$
AMPO	3(13292)	Amplitude at the end of the reactivity time step $N(t_i^n)$
AMPVA(3)	3(13296)	Last three values of the logarithm of the amplitude, $1n[N(t_{i-3}^n)]$ $1n[N(t_{i-2}^n)], 1n[N(t_{i-1}^n)]$ AMPVA is used in an interpolation scheme to produce AMPCO
AMPYIN	3(13295)	Integral of the amplitude, using the Modified (final sweep) values of N,

$$\int_0^t N(t) dt$$

BASET	2(11352)	Base temperature ( $T_0$ ) of all isotopes, and therefore of all mixtures
BCD(10)	2(11353)	Problem title card, stored in 10A8 format
BETA(6)	3(13302)	The current delayed-neutron fraction ( $\beta$ )
BETCO(3,6)	3(13326)	Coefficients of the $\beta / \Lambda$ parabola $a_1, a_2, a_3$ (one set for each delayed family), used to interpolate as $(\beta_s / \Lambda)(t) = a_1 + a_2(t - t_{i-1}^n) + a_3(t - t_{i-1}^n)^2$
BETVA(3,6)	3(13308)	Last three values (for each delayed family) of beta divided by generation time, $(\beta_s / \Lambda)(t_i^{n-2}), (\beta / \Lambda)(t_i^{n-1}), (\beta_s / \Lambda)(t_i^n)$
BUCK(30,20)	2(391)	Group- and region-dependent buckling values
C(150,6)	3(13362)	Point- and family-dependent delayed-neutron precursor densities ( $C_s(\vec{r})$ )
CALMI(100)	2(12263)	Last calculated value of the driving function while the I driving function is in use. While the driving function is not in use, CALMI = 1
CB(19,6)	3(14262)	Family-dependent inner boundary values (for regions 2 through NOR) of the delayed-neutron precursor densities
CHID(30,6)	2(11166)	Group- and family-dependent delayed-neutron spectra ( $\chi_{sg}^d$ )
CHIEX(30)	2(1330)	Group-dependent external source spectrum. Entered only if KUSOR $\geq 2$
CHIP(30)	2(1490)	Group-dependent prompt-neutron spectrum ( $\chi^p$ )

CNORM	3(13275)	Constraint-condition normalization factor, set equal to 1.0
COCAP(20)	2(12083)	Regionwise coolant heat capacities = $\frac{1}{\rho_c} \left( \frac{cm^3 \times ^\circ K}{W \times sec} \right)$ Currently unused
COT(20)	2(12023)	Regionwise coolant inlet temperatures ( $^\circ K$ ). Currently unused.
COV(20)	2(12003)	Regionwise coolant velocities ( $v_c$ ) in cm/sec. Currently unused.
CRAM(300)	2(11)	Dummy floating-point container array, used to pass local equivalences from one routine to another and as scratch.
CRAT	3(13276)	Hollerith name of cross-section file (A5).
DECAY	2(11345)	Family-dependent decay constants ( $\lambda_f$ ).
DELR(20)	3(13071)	Interval length in each region ( $\Delta r$ ).
DESK	2(3)	Desired k to be searched. If DESK = 0, k is set to 1.0 by the code.
DH(20)	2(1380)	Region-dependent $\Delta H$ values. currently unused; set to zero.
DIF(30,20)	3(11121)	Group- and region-dependent diffusion coefficient. $D^R$ is calculated by the code as $\frac{1}{3\sigma_g^{tr}}$ .
DOPCO(30,8,6)	2(8286)	Group and internal mixture-dependent Doppler coefficients. Defined for fuel mixtures only, and used to update the temperature-dependent capture and/or fission cross sections. The dimension 6 represents $a_1, a_2, a_3$ (capture coefficients) and $a_1, a_2, a_3$ (fission coefficients).

DT	3(13281)	Length of the current reactivity step ( $\Delta t_i^n$ ).
DT1	3(13282)	Length of the last reactivity step ( $\Delta t_{i-1}^n$ ).
DT2	3(13283)	Length of the second-to-least reactivity step ( $\Delta t_{i-2}^n$ ).
DTBOLT	3(13284)	Length of the last shape-function step ( $\Delta t_{i-1}^B$ ).
DTMAX(5)	3(13285)	<p>Maximum allowable shape-function time-step lengths. The dimension 5 is as follows:</p> <ol style="list-style-type: none"> <li>1. <math>\Delta t_{\max}</math> for the shape-function criterion (Eq. 59).</li> <li>2. <math>\Delta t_{\max}</math> for the delayed-neutron source criterion (Eq. 60)</li> <li>3. <math>\Delta t_{\max}</math> for the coolant-velocity criterion. Currently unused.</li> <li>4. <math>\Delta t_{\max}</math> for the regionwise-reactivity criterion (Eq. 61).</li> <li>5. <math>\Delta t_{\max}</math> for the next driving-function control. See Section V.</li> </ol>
DUMPT	2(10)	The dump interval (if KUDUMP = 1 or 3). The point-kinetics dump is taken at all shape-function steps and all reactivity steps, plus at times equal to multiple of DUMPT.
DY(20)	2(1420)	The region-dependent $\Delta Y$ values. Currently unused; set to zero.
EIGCUR	3(13094)	The current eigenvalue of the shape solution during solution iterations.
EIGEN	3(13092)	The final converged k-effective of the static system ( $k_0$ ). (The adjoint eigenvalue.)
EIGOLD	3(13093)	Eigenvalue of the previous shape function iteration.

EPS(20)	2(1440)	The convergence-criterion container array. A total of 13 epsilons are currently defined (see Table V).
EPSIN	2(1)	Source-convergence criterion for shape solution
EPSOUT	2(2)	Search-convergence criterion for shape solution.
EXCO(3)	3(14379)	Coefficients of the external source parabola, $a_1, a_2, a_3$ . Used in point kinetics to interpolate $S_{EX}(t)$ as $S_{EX}(t) = a_1 + a_2(t - t_{i-1}^n) + a_3(t - t_{i-1}^n)^2$
EXSOR(150)	2(1161)	Point-dependent external sources.
EXSORB(19)	2(1311)	Boundary values of the external Sources.
EXVA(3)	3(14376)	Last three values of the integrated external source $S_{EX}(t_{n-2}), S_{EX}(t_{n-1}), S_{EX}(t_n)$ . Used in an interpolation scheme to produce EXCO.
FINT	2(7)	Final reactor time when the calculation is to end (if KEND = 0).
FISOR(150)	2(991)	Point-dependent starting fission source. On input; for KUSOR = 0 or 2, enter NOR values (if 0, the code assumes a source of 1.0), which are smeared over points. For KUSOR = 1 or 3, enter the pointwise values, with the inner boundary values entered into FISORB.
FISORB(19)	2(1141)	Boundary values of the starting fission source. If KUSOR = 0 or 2, this array is filled by the code. If KUSOR = 1 or 3, enter the inner boundary values for regions 2 through NOR.
FUCAP(20)	2(12103)	Regionwise fuel heat capacities,

		$\frac{1}{\rho c}, \left( \frac{cm^3 \times ^\circ K}{W \times sec} \right)$ . Used by the fuel-temperature routine.
H(20)	2(1360)	Region-dependent limits of the transverse integral in the H direction. Currently unused; set to 1.0E11.
HETCON(20)	2(12043)	Regionwise fuel-coolant heat-transfer time constants, in $sec^{-1}$ . Currently unused.
ID1	1(506)	XLIBIT cross-section file (CDC-3600 only) or BCD card-image file LUN number. Set by the code to 1.
ID2	1(507)	QX1 cross-section file LUN number. Set by the code to 2.
ID3	1(508)	LUN number of scratch file for amplitude-shape iteration. Set by the code to 3.
ID4	1(509)	LUN number for driving-function data scratch file. Set by the code to 4.
ID5	1(510)	Point-kinetics dump-file LUN number. Set by the code to 8. The point-kinetics dump is temporarily stored here and rewritten onto ID3 at the end of the run.
ID6	1(511)	Shape dump-file LUN number. Set by the code to 9. The shape dump is temporarily stored here and rewritten onto ID3 at the end of the run.
ID7	1(512)	Scratch file LUN number. Set by the code to 10.
IDS	1(505)	Scratch file LUN number used to store previous shape function. Set by the code to 50.
IFLAG	1(523)	Problem-condition flag: 0 denotes real static solution is running; 1 denotes

the adjoint solution is running, as well as first time flag for the dynamic solution; 2 denotes the final dynamic solution, and first time static pass.

INDEX(16)	1(169)	The internal mixture numbers. If I is the external mixture number (assumed from the order of appearance on input), then the internal number is INDEX(I). Internal numbers 1-8 are reserved for fuels, and 9-16 for nonfuels.
ITIN	1(520)	Flux iteration counter.
ITOUT	1(521)	Search iteration counter.
JAM(70)	1(22)	Dummy fixed-point container array. Used to pass local equivalences from one routine to another, or used as scratch.
KEND	1(10)	Final time flag. If 0, the problem will end when $t = \text{FINT}$ . If 1, the problem will end when $t = t_f$ , where $N(t_f) = \text{AMPLIM}$ and/or $\rho(t_f) = \text{ROLIM}$ .
KIND	1(2)	Search flag: 0 for k search (no search); 1 for dimension search (reactor size not fixed); 2 for composition search; 3 for dimension search (reactor size fixed); 4 for buckling search.
KONIN	1(4)	Inner boundary condition: 0 for zero gradient; 1 for zero flux; 2 for logarithmic derivative with extrapolation length input (see below); 4 for logarithmic derivative with extrapolation length calculated by the code (Ref. 21).
KONOUT	1(5)	Outer boundary condition: 0 for zero flux; 1 for zero gradient; 2 for logarithmic derivative with extrapolation

		length input (see below); 4 for logarithmic derivative with extrapolation length calculated by the code (Ref. 21).
KREGS(20)	1(132)	NOKREG search region numbers.
KUAP	1(16)	Adjoint flag. If 1, do not print the adjoint shape function; if 0, print.
KUBUCK	1(6)	Buckling flag: 0 for constant height or radius; 1 for region-dependent height or radius; 2 for group-dependent buckling; 3 for region- and group-dependent buckling.
KUCHEB	1(18)	Dynamic shape-debug print flag. If > 0, print the Chebyshev debug data.
KUDUMP	1(19)	Dump flag: 0 for no dump; 1 for point-kinetics dump; 2 for shape dump; 3 for both point-kinetics and shape dump. File 3 must be saved if dump is requested.
KUDYS	1(11)	Shape-function time-derivative flag: 0 for quasi-static model; 1 for improved quasi-static model (derivative included); 2 for factorized model with shape-function extrapolation. (2 is recommended.)
KUIP	1(14)	Input print flag: 0 for normal input print; 1 for adding initial cross-section print; 2 for adding final cross-section print; 3 for adding both of the above; 4 for all of the above, plus the cross-section print at shape-recalculation step.
KUMP	1(17)	Composition print flag. If 1, print the mixture dependent composition data at each reactivity time step; if 0, do not print.
KUOP	1(15)	Output print flag. If 0, print the shape function at each step; if 1, print the

		shape function only at $t = 0$ and $t =$ final time; if 2, print the shape function and precursors at each step.
KUPK	1(21)	Set equal to 1 to run point kinetics option.
KUSOR	1(7)	Source flag: 0 for fission-source guess input by region; 1 for fission-source guess by point; 2 for fission-source guess by region plus pointwise external source; 3 for fission-source guess by point plus external sources. A value greater than 3 identifies a pulse problem with first-collision distribution (see Section III.C.5). Set KUSOR equal to 3 plus the driving-function number in which the time distribution of the pulse is specified.
KUWIG	1(20)	WIGLE punch flag. If 1, punch the starting points for the WIGLE code (two-group problem only); if 0, do not punch.
LABEL(16)	1(153)	The mixture label for each mixture. (One of FISS, FERT, COOL, CLAD, CONT, STRC is read off the mixture data, and stored for each mixture.)
MAB(20)	1(525)	Mesh-point number at the outer boundary of each region.
MAKE	1(1)	Geometry flag: 1 for slab; 2 for cylinders; 3 for spheres.
MAXIN	1(8)	Flux-iteration limit. If this is 0 on input, it is set by the code to 100.
MAXORD	1(522)	The order of the point-kinetics time steps. A normal time step ( $\Delta t_i^n$ ) is divided into $2^{n-1}$ subintervals, where $n$ is the value stored in variable MAXORD.
MAXOUT	1(9)	Search-iteration limit. If this is 0 on

		input, it is set by the code to 10.
MFLAG(16,20)	1(185)	The region-dependent mixture flag: +1 denotes a diluent mixture; -1 denotes a fuel mixture (these two relevant only to a composition search); 0 denotes a neutral mixture; 2 denotes the mixture is unused in this region.
MIR(20)	1(112)	The composition number for each region.
NAMEX	1(152)	Currently unused.
NEAT	1(13)	Heat-transfer flag. If 0, the fuel-temperature calculation will not be done; if 1, it will be done.
NINT(20)	1(92)	Number of mesh intervals in each region.
NIX	1(124)	The internal trouble cue: 0 denotes no trouble; 1 denotes a problem fault (a dump is given and computation stops). If NIX = -1, the criticality search has converged; 2 denotes unrecoverable error.
NOC	1(519)	Number of compositions.
NOD	1(517)	Number of downscatters. The maximum number is stored after the cross sections are read. The internal loop index is L.
NOF	1(516)	Number of delayed families. The internal loop index is K.
NOG	1(513)	Number of energy groups. The internal loop index is J.
NOGO(100)	1(545)	Status word for driving functions. If 0, function has not been turned on. If 1, it is active. If 2, it has been turned off.

NOKREG	1(3)	Number of search regions.
NOM	1(518)	Number of mixtures.
NOP	1(515)	Number of mesh points. Equal to the Number of intervals plus 1. The internal loop index is N.
NOR	1(514)	Number of spatial regions. The internal loop index is M.
NUMI	1(12)	Number of driving functions in the problem.
OMEGI(30)	2(331)	Group-dependent inner-boundary extrapolation lengths ( $\omega$ ) (if KONIN = 2). These values are negative.
OMEGO(30)	2(361)	Group-dependent outer-boundary extrapolation lengths ( $\omega'$ ) (if KONOUT = 2). These values are positive.
PHI(30,150)	3(1)	Group- and point-dependent real shape solution $\psi_g(x,t)$ .
PICT(20)	2(12123)	Regionwise pin-conduction terms ( $a^2 / 8K$ in $cm^3 \times ^\circ K / W$ ). Currently unused.
PIM	3(13091)	A code-calculated geometrical factor: 1.0 for slabs, 2.0 for slabs with the gradient zero at the inner boundary ( $\Phi_{R=0} = 0$ ), $2\pi$ for cylinders, $4\pi$ for spheres.
PIST(20)	2(12143)	Regionwise-pin surface terms, ( $a^2 / 2H$ in $cm^3 \times ^\circ K / W$ ). Currently unused.
POW	2(5)	Desired power in watts. If POW = 0, one watt is assumed by the code.
POWIN(20)	3(13175)	Regionwise power integrals. Calculated

		by the code as
		$\int_V \int_E \sum_f \psi dEdV$
PREC(6)	3(13356)	Family-dependent integrated precursor densities ( $\eta_s$ ).
PROL	3(13352)	Current prompt-neutron generation time ( $\Lambda$ ).
PROLVA(3)	3(13353)	The last three values of generation time: $\Lambda(t_{i-2}^n), \Lambda(t_{i-1}^n), \Lambda(t_i^n)$ . PROLVA is used in an interpolation scheme to produce the current generation time $\Lambda(t)$ . (Needed only for purposes of editing the amplitude-function data.)
R(150)	3(12921)	The radius at each mesh point ( $\bar{r}$ ).
REFAC(20)	2(12063)	Regionwise radial reduction factors for effective temperature calculations. Used by the fuel-temperature routine.
REGRO(20)	3(13195)	Regionwise reactivity at the last shape-function step.
REGROT(20)	3(13215)	Current regionwise reactivity.
REGSH(20)	3(14382)	Regionwise group- and region-integrated flux shape function at the last shape-function step.
REGSHT(20)	3(14402)	Current integrated flux shape function.
RESDUE	3(13344)	Initial steady-state reactivity residue ( $\rho(0)$ ). This residue is subtracted from all reactivities, so that $\rho(t) = \rho'(t) - \rho(0) + (k_0 - 1) / k_0$
RO	3(13345)	Current reactivity $\rho(t)$ .
ROCO(3)	3(13349)	Coefficients of the $\rho / \Lambda$ parabola, $a_1, a_2, a_3$ , used to interpolate as $\frac{\rho}{\Lambda}(t) = a_1 + a_2(t - t_{i-1}^n) + a_3(t - t_{i-1}^n)^2$

ROLIM	2(8)	Final reactivity value (if KEND = 1). Calculation ends when $\rho(t_f) = \text{ROLIM}$ .
ROUT(20)	2(311)	Outer radius of each region.
ROVA(3)	3(13346)	Last three values of reactivity over generation time: $\frac{\rho}{\Lambda}(t_i^{n-2}), \frac{\rho}{\Lambda}(t_i^{n-1}), \frac{\rho}{\Lambda}(t_i^n)$
RZERO	2(4)	Radius at the inner boundary. This value is later loaded into R(1).
SCAT(331,20)	3(4501)	Region-dependent downscatter array. The layout of this array is identical to SIGS, except SCAT is now region- dependent, rather than mixture- dependent.
SIGC(30,16)	2(6846)	Group- and mixture-dependent sigma capture array. Read off the cross- section tape, but can be altered with input cards. The relative address in SIGC of $\sigma_g^c$ for internal mixture m group g is $A = 30(m-1) + g$ .
SIGF(30,8)	2(7806)	Group- and mixture-dependent sigma fission array. Defined for fuel mixtures only. Read off the cross-section tape, but can be altered with input cards. The relative address in SIGF of $\sigma_g^f$ for internal mixture m group g is $A = 30(m-1) + g$ .
SIGN(30,8)	2(8046)	Group- and mixture dependent prompt nu-sigma fission array. Defined for fissionable mixtures only. Read off the cross-section file, but can be altered with input cards. The relative address in SIGN of $\nu P \sigma_g^f$ for internal mixture m group g is $A = 30(m-1) + g$ .
SIGT(30,16)	2(7326)	Group- and mixture-dependent sigma transport array. Read off the cross- section file, but can be altered with

input cards. The relative address in SIGT of  $\sigma_g^{tr}$  for internal mixture  $m$  group  $g$  is  $A = 30(m-1) + g$ .

SIGS(331,16)	2(1550)	<p>Mixture-dependent downscatter array. Read off the cross-section file, but can be altered with input cards. The order of the downscatters, for a particular mixture, is as follows: 0, <math>\sigma^{2\leftarrow 1}, \sigma^{3\leftarrow 1}, \sigma^{3\leftarrow 2}, \sigma^{4\leftarrow 1}, \sigma^{4\leftarrow 2}, \sigma^{4\leftarrow 3}, \sigma^{5\leftarrow 1}, \dots, \sigma^{15\leftarrow 14}, \sigma^{16\leftarrow 1}, \sigma^{16\leftarrow 2}, \dots, \sigma^{16\leftarrow 15}, \sigma^{17\leftarrow 2}, \dots, \sigma^{17\leftarrow 16}, \sigma^{18\leftarrow 3}, \sigma^{18\leftarrow 4}, \dots, \sigma^{30\leftarrow 29}</math>.</p> <p>This layout uses 331 locations per mixture. The relative address in SIGS, A, of <math>\sigma_{gg'}</math>, for internal mixture number is as follow:  <i>for</i> <math>g \leq 15 : A = 331(m-1) + 1</math>  <math display="block">+ \sum_{k=3}^g (k' - 2) + g',</math> <i>for</i> <math>g \geq 16 : A = 331(m-1) + 106</math>  <math display="block">+ 15(g-16) + g' - (g-16);</math> <i>where</i> <math>1 \leq g, g' \leq 30, g-15 \leq g' &lt; g</math></p>
SORCHI(30)	2(1520)	Emission spectrum of the pulse in first-collision pulsed-source problems.
SORD(20)	3(13235)	Regionwise delayed precursor source at the last shape-recalculation step.
SORDT(20)	3(13255)	Current regionwise precursor source.
TBOLT	3(13280)	The time at the last shape-recalculation step ( $t_{i-1}^B$ ).
TCUR	3(13277)	The current-calculation time.
TMAX	3(13279)	The time at the end of the current-reactivity recalculation step ( $t_i^n$ ).
TMIN	3(13278)	The time at the start of the current-reactivity recalculation step ( $t_{i-1}^n$ ).

TMULT	2(6)	First time-step multiplier. The initial time step will be of length TMULT times the generation time. If no value is entered, TMULT = 1.
TOTR(30,20)	3(12321)	The group- and region-dependent total removal array.
TRAD(20)	3(13095)	Regionwise geometrical factor for volume integrals. Unused; set to 1 internally.
TRAN(20)	3(13135)	Regionwise geometrical factor for volume integrals. Unused; set to 1 internally.
TRAV(20)	3(13155)	Regionwise geometrical factor for volume integrals. Unused; set to 1 internally.
VALTR(100)	2(12163)	The driving-function trigger value. When the driving function is active. VALTR contains the actual time at which the driving function was initiated.
VAT(16,20,2)	2(11363)	Mixture- and region-dependent volume fraction-temperature array. VAT(I,J,1) is the volume fraction and VAT(I,J,2) the temperature of mixture I in region J.
VEL(30)	2(1460)	Group velocities ( $v_g$ ). Read off the cross-section file, but can be altered with input cards.
Y(20)	2(1400)	Region-dependent limits of the transverse integral in the Y direction. Currently unused; set to zero.
YIELD(30,6,8)	2(9726)	The group-, family-, and mixture-dependent delayed-neutron precursor yield per fission.

## ACKNOWLEDGMENTS

The authors gratefully acknowledge the continuing interest and support of Drs.H.H.Hummel and G.J.Fischer throughout this work. Dr.E.L.Fuller provided several suggestions for improving the time-step selection logic and detected many program bugs during the later stages of code testing. Many helpful suggestions were made by Dr.G.K.Leaf, particularly in the area of acceleration and convergence of the shape-function solution. Mrs.Marjorie A.Luebs prepared the original manuscript. Finally, the authors wish to thank the members of the ANL-AMD Computer Center for their support during development of the code.

## REFERENCES

1. K. Ott and J. Madell, *Quasistatic Treatment of Spatial Phenomena in Reactor Dynamics*, Nucl. Sci. Eng. 26, 563 (1966).
2. A. F. Henry, *The Application of Reactor Kinetics to the Analysis of Experiments*, Nucl. Sci. Eng. 3, 52 (1958).
3. K. Ott, D. Meneley, and E. Wiener, "Quasistatic Treatment of Space Dependent Reactor Transients," *Reactor Physics Division Annual Report, July 1, 1965 to June 30, 1966*, ANL-7210, pp. 370-373 (Dec 1966).
4. D. A. Meneley, K. Ott, and E. S. Wiener, "Space-Time Kinetics—The QX1 Code," *Reactor Physics Division Annual Report, July 1, 1966 to June 30, 1967*, ANL-7310, pp. 471-476 (Jan 1968).
5. D. A. Meneley, K. Ott, and E. S. Wiener, "Accuracy of Factorizing Methods in Spatial Kinetics," *Reactor Physics Division Annual Report, July 1, 1967 to June 30, 1968*, ANL-7410, pp. 391-397 (Jan 1969).
6. D. A. Meneley, K. Ott, and E. S. Wiener, "Further Development of the Quasistatic Neutron Kinetics Model," *Reactor Physics Division Annual Report, July 1, 1967 to June 30, 1968*, ANL-7410, pp. 398-400 (Jan 1969).
7. D. A. Meneley, K. Ott, and E. S. Wiener, *influence of the Shape Function Time Derivative in Spatial Kinetics*, Trans. Am. Nucl. Soc. 11(1), 225 (1968).
8. D. A. Meneley, K. O. Ott, *Spectral Effects in Liquid-Metal Fast Breeder Reactor Transients*, Trans. Am. Nucl. Soc. 12(2), 706 (1969).
9. K. O. Ott and D. A. Meneley, *Accuracy of the Quasistatic Treatment of Spatial Reactor Kinetics*, Nucl. Sci. Eng. 36, 402 (1969).
10. B. J. Toppel, *The Argonne Reactor Computation (ARC) System*, ANL-7332 (Nov 1967).
11. D. A. Meneley, G. K. Leaf, A. J. Lindeman, T. A. Daly, and W. T. Sha, "A Kinetics Model for Fast Reactor Analysis in Two Dimensions," *Proc. Symposium on Dynamics of Nuclear Systems, Tucson, Arizona, March 23-25, 1970* (in publication).
12. *Reactor Development Program Progress Report, July 1969*, ANL-7595, pp. 5-7.
13. *Reactor Development Program Progress Report, August 1969*, ANL-7606, pp. 4-6.

14. *Reactor Development Program Progress Report, September 1969*, ANL-7618, pp. 1-4.
15. *Reactor Development Program Progress Report, October 1969*, ANL-7632, pp. 1-4.
16. *Reactor Development Program Progress Report, December 1969*, ANL-7655, pp. 1-4.
17. *Reactor Development Program Progress Report, February 1970*, ANL-7669, pp. 11-13.
18. *Reactor Development Program Progress Report, June 1970*, ANL-7705, pp. 1-3.
19. *Reactor Development Program Progress Report, August 1970*, ANL-7737, pp. 5-8.
20. *Reactor Development Program Progress Report, November 1970*, ANL-7758, pp. 7-9.
21. H. P. Flatt and D. C. Baller, *Aim-5, A Multigroup, One-Dimensional Diffusion Equation Code*, NAA-SR-4694 (1960).
22. S. D. Sparck, *XLIBIT: ANL Cross-section Library Code*, ANL-7112 (Feb 1966).
23. D. A. Meneley, "The Effective Delayed Neutron Fraction in Fast Reactors," *Reactor Physics Division Annual Report, July 1, 1967 to June 30, 1968*,
24. A. Travelli, "A New Formulation of Multigroup Microscopic Cross Sections," *Reactor Physics Division Annual Report, July 1, 1967 to June 30, 1968*, ANL-7410, pp. 413-421 (Jan 1969).
25. B. J. Toppel, A. L. Rago, and D. M. O'Shea, *MC<sup>2</sup>, A Code to Calculate Multigroup Cross Sections*, ANL-7318 (June 1967).
26. L. K. Volodka, "PROGRAM MOVER: Point Kinetics Algorithm," *Reactor Physics Division Annual Report, July 1, 1966 to June 30, 1967*, ANL-7310, pp. 492-493 (Jan 1968).